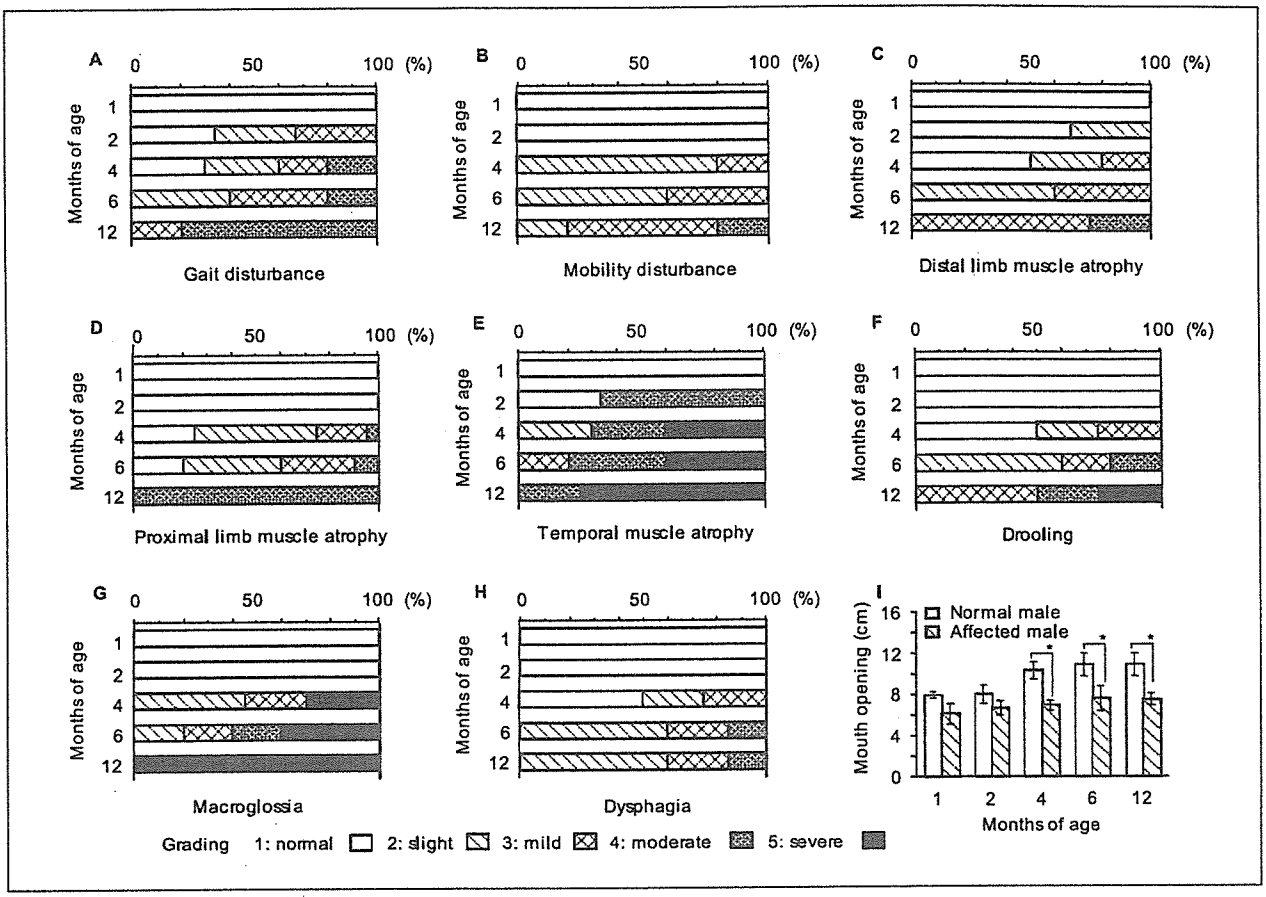

Figure 4. Evaluation of clinical phenotypes in affected G3 male dogs. The evaluation of each clinical sign is shown in **A-H**: (**A**) gait disturbance, (**B**) mobility disturbance (**C**) distal limb, (**D**) proximal limb, (**E**) and temporal muscle atrophy, (**F**) drooling, (**G**) macroglossia, and (**H**) dysphagia at the ages of 1, 2, 4, 6, and 12 months. The severity of each sign in affected G3 dogs was classified into five grades as described in Materials and Methods and Table. The percentage of affected G3 dogs in each grade was calculated for each month of age. (**I**) Maximum mouth opening in normal and affected G3 male dogs at the ages of 1, 2, 4, 6, and 12 months. Bar: mean ± S.E.; $^{*}p < 0.05$.

diaphragma muscle in an affected G3 male disclosed marked variation in fiber size and increase in fibrosis and necrotic fibers (**Fig. 5F**).

The diameter of the fibers in the anterior tibial muscle increased with age in normal G3 males (**Fig. 6A-C**), while the muscle in the sacrificed, affected G3 male at 3 days of age showed slight fiber size variation and some necrotic fibers (**Fig. 6D**). The findings were not different from those in an affected G3 male that died at 1 day of age (data not shown). At the age of 2 months, the tibial muscle from an affected G3 male displayed an increase in the number of necrotic fibers, invasion of inflammatory cells, and a slight proliferation of the interstitial tissues (**Fig. 6E**). At the age of 6 months, marked fiber size variation, increase in the interstitial fibrosis, and hypertrophied or centrally nucleated fibers were observed (**Fig. 6F**).

In macroscopic examinations, an affected G3 male at the age of 12 months had severe hypertrophy of the tongue, genioglossus, and geniohyoideus muscles (**Fig. 7B**) as compared with those in a normal male (**Fig. 7A**). In the tongue muscle, there were many hypertrophied fibers and opaque fibers (**Fig. 7D**), as compared with those in the normal male (**Fig. 7C**).

Discussion

In this report, we described the major clinical and histopathological phenotypes of beagle-based dystrophic dogs, $CXMD_J$, that carried the same *dystrophin* gene mutation as CXMD dogs. We

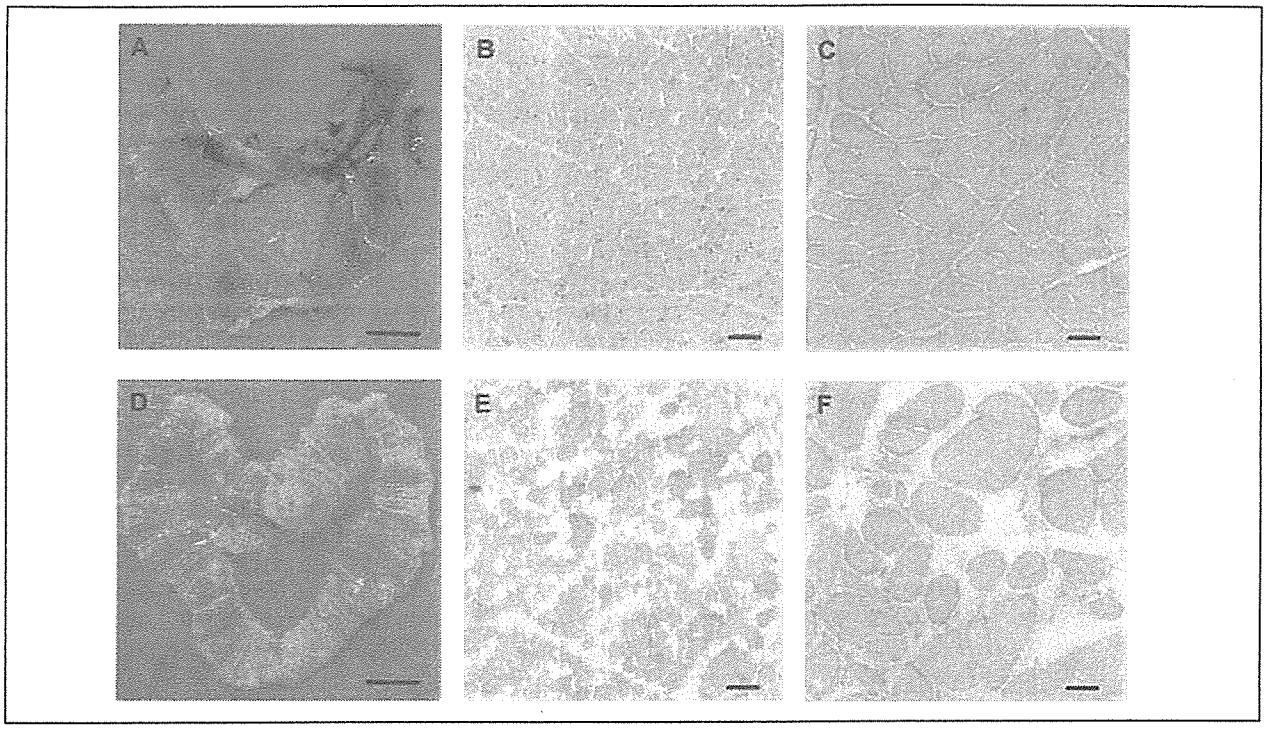

Figure 5. Macroscopy and histopathology of diaphragm muscles. Diaphragm of a normal G3 male dog that died at 1 day of age (**A**) and an affected G3 male dog that was sacrificed at 3 days of age (**D**). Bar = 1 cm. H&E staining of cross-sections of diaphragm muscles from normal G3 male at 3 day of age (**B**) and at 6 months of age (**C**), and from affected G3 males that was sacrificed at 3 days of age (**E**) and 6 months of age (**F**). Bar = 50 μm.

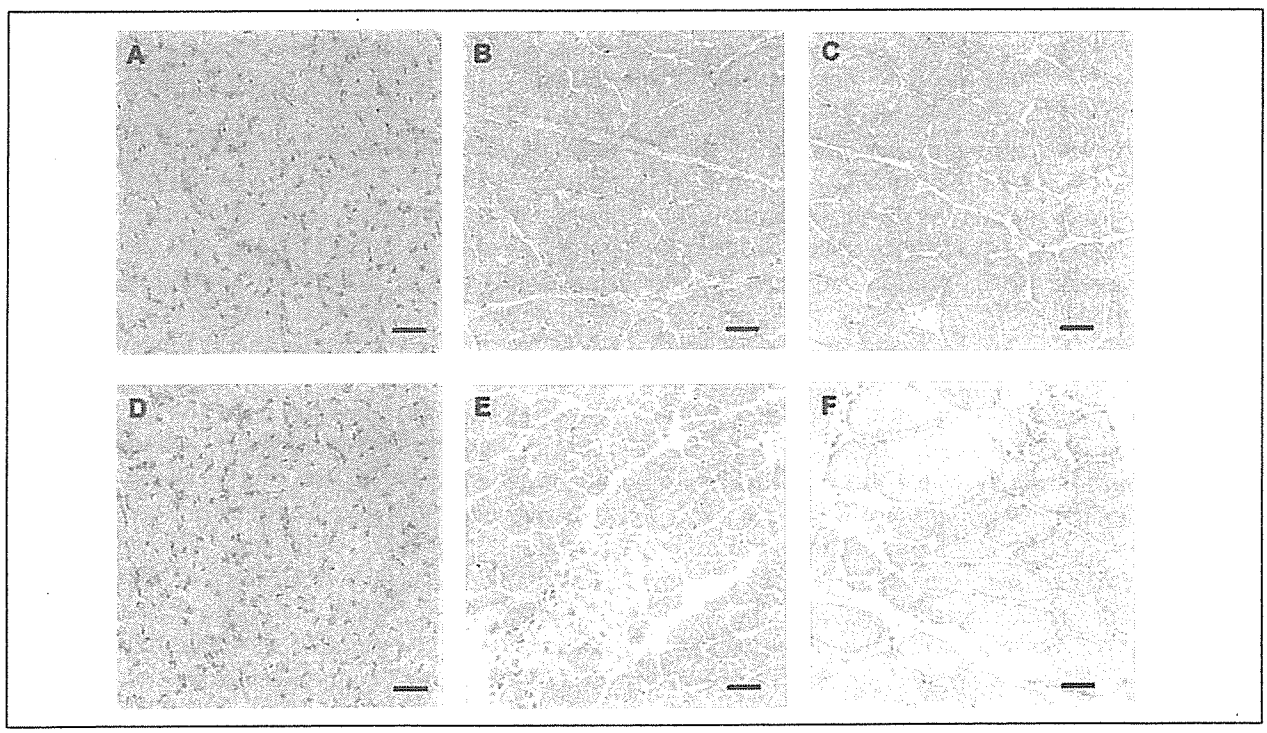

Figure 6. Histopathology of anterior tibial muscles. H&E staining of cross-sections of anterior tibial muscles from normal G3 male at 3 days of age (**A**), 2 month of age (**B**), and 6 months of age (**C**), and from affected G3 male at 3 days of age (**D**), 2 month of age (**E**), and 6 months of age (**F**). Bar = 50 μm.

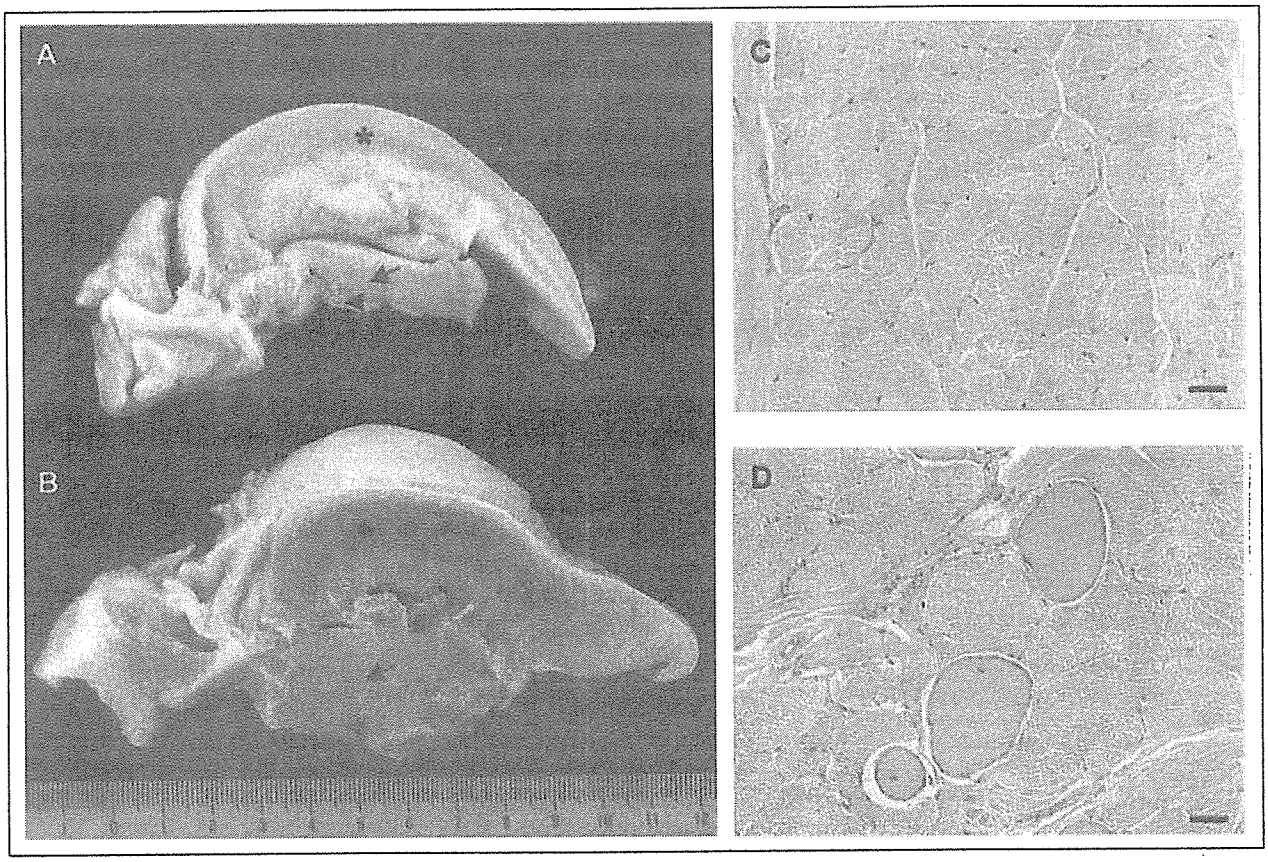

Figure 7. Macroscopy and histopathology of tongue and sublingual muscles. Tongue (asterisk), genioglossus (arrow) and geniohyoideus (arrowhead) muscles in a normal G3 male (**A**) and an affected G3 male (**B**) at 12 months of age. Bar = 1 cm. H&E staining of cross-sections of the tongue muscle from a normal G3 male (**C**) and an affected G3 male (**D**) at 12 months of age. Bar = 50 μm.

dealt mainly with the third generation of dystrophic dogs, G3, when they still have mixture of both beagle and golden retriever backgrounds. However, the size of G3 $CXMD_J$ was smaller and easier to handle than golden retriever-based CXMD dogs [16].

The serum CK levels in affected G3 dogs reached two peaks during the course: the first peak occurred immediately after birth and the second peak at two months after birth. This particular pattern of serum CK levels was also seen in G3 carrier females, although the increase was quite small. Previous researchers have reported that serum CK levels in CXMD dogs were much higher than those in normal littermates shortly after birth [15, 17] and had another peak at 6 to 8 weeks after birth [15]. The profiles of serum CK levels in our dystrophic G3 dogs corresponded well with these reports.

The elevation of serum CK levels in G3 affected and carrier female dogs shortly after birth may be a result of acute generalized muscle damage after the stress of whelping. It is very important to note that 32.3% of affected G3 male pups had died by 3 days of age, and the rate was significantly higher than that of normal dogs. Actually, it has been reported that 28.0% or 45.5% CXMD pups died with a neonatal fulminant form within the first 2 weeks after birth [15, 18]. Although the cause has not been fully elucidated, acute respiratory failure might be associated with the pathogenesis of the early death because involvement of the diaphragm muscle was seen in neonatal fulminant CXMD pups [19] as well as in affected G3 dogs at three days after birth (**Fig. 5E**). The stress of whelping is one factor that may exacerbate involvement of the diaphragm. Moreover, Nguyen et al. reported selective involvement of the diaphragm muscle in neonatal CXMD pups, and they found that anterior tibial muscle damage was not more severe than that of the diaphragm muscle [19]. In affected G3 dogs, a similar selec-

tive pattern was observed at the neonatal stage (**Fig. 5E and 6D**). It is very intriguing to note that genetic variation of sire may influence on the neonatal phenotypes of dystrophic dogs, since the same carrier produced different types of dystrophic pups: neonatal fulminant or less severe dystrophic pups.

The serum CK levels in G3 affected and carrier female dogs increased again at 2 months of age. Onset of clinical symptoms, such as gait and mobility disturbances and muscle atrophy, were definite from 2 months of age in affected G3 males (**Fig. 4A-E**). The onset of the disease might be closely related to the second peak of serum CK that we found in affected G3 dogs. The period of around 2 months of age corresponds to canine socialization for developing spontaneous activities after the weaning [20]. It is, therefore, possible that the increase in activity of pups may effect on an elevation of serum CK levels and on the onset of clinical symptoms. Valentine et al. reported that the age of onset of muscle involvement in CXMD dogs was from 8 to 10 weeks of age [4, 15]. Those results were largely consistent with the data on our affected G3 dogs. On the other hand, they also reported that the disease severity in affected beagle-crossed dogs was milder than that in CXMD dogs around the age of 8 weeks [15]. The same criteria could be required to evaluate and compare affected G3 dogs with CXMD dogs.

The feeding difficulty and jaw joint contracture were apparent from 4 months of age (**Fig. 4F-I**). At 6 months of age, histopathological findings of diaphragm (**Fig. 5F**) and anterior tibial (**Fig. 6F**) muscles in affected G3 male dogs were compatible with those in CXMD dogs at 6 months of age [21]. All affected G3 dogs at the age of 12 months showed severe macroglossia and hypertrophy of the sublingual muscles (**Fig. 7B**). Degeneration of tongue muscle fibers has been noted as early as the neonatal stage in CXMD [18, 19], although we have not confirmed that. Elucidation of tongue and sublingual muscle involvement in dystrophic dogs is indispensable, because dysphagia is now one of the major symptoms in older DMD patients [22, 23].

Finally, we here showed the characteristics of G3 CXMD$_J$, and especially emphasized the particular change of serum CK levels with age, not only in G3 CXMD$_J$ but also in female carrier dogs. The extremely high CK values we found in neonatal dystrophic dogs may reflect respiratory muscle damage due to stress during whelping. These findings in G3 CXMD$_J$ dogs were similar to those in CXMD dogs; therefore, CXMD$_J$ is a useful model for investigation of the pathogenesis of and development of therapies for dystrophin-deficient muscular dystrophy, DMD.

Acknowledgements

We thank Naoko Yugeta, D.V.M. (School of Veterinary Medicine, Azabu University) for advising on the healthy care of dogs and also thank Hideki Kita, Shinichi Ichikawa, Yumiko Yahata, and Kazue Kinoshita (JAC, Inc., Tokyo) for keeping of dogs. This study was supported by Grants-in-Aid for Research on Nervous and Mental Disorders (13B-1, 16B-2) and Health Sciences Research Grants for Research on Psychiatric and Neurological Diseases and Mental Health (H12-kokoro-025, H15-kokoro-021), the Human Genome and Gene Therapy (H13-genome-001, H16-genome-003) from the Ministry of Health, Labor and Welfare of Japan, and Grants-in-Aid for Scientific Research from the Ministry of Education, Science, Sports and Culture of Japan (to Y.S. and S.T.).

References

1. Moser H. Duchenne muscular dystrophy: pathogenetic aspects and genetic prevention. Hum Genet 1984;66:17-40.
2. Koenig M, Hoffman EP, Bertelson CJ, et al. Complete cloning of the Duchenne muscular dystrophy (DMD) cDNA and preliminary genomic organization of the DMD gene in normal and affected individuals. Cell 1987;50:509-17.
3. Bulfield G, Siller WG, Wight PA, et al. X chromosome-linked muscular dystrophy (*mdx*) in the mouse. Proc Natl Acad Sci USA 1984;81:1189-92.
4. Valentine BA, Cooper BJ, Cummings JF, et al. Progressive muscular dystrophy in a golden retriever dog: light microscope and ultrastructural features at 4 and 8 months. Acta Neuropathol (Berl) 1986;71:301-10.
5. Cooper BJ, Winand NJ, Stedman H, et al. The homologue of the Duchenne locus is defective in X-linked muscular dystrophy of dogs. Nature 1988;334:154-6.
6. Kornegay JN, Tuler SM, Miller DM, et al. Muscular dystrophy in a litter of golden retriever dogs. Muscle Nerve 1988;11:1056-64.
7. Valentine BA, Winand NJ, Pradhan D, et al. Canine X-linked muscular dystrophy as an animal model of Duchenne muscular dystrophy: a review. Am J Med Genet 1992;42:352-6.
8. Shelton GD, Engvall E. Canine and feline models of human inherited muscle diseases. Neuromuscul Disord 2005; 15:127-38.
9. Shimatsu Y, Katagiri K, Furuta T, et al. Canine X-linked muscular dystrophy in Japan (CXMD$_J$). Exp Anim 2003;52:93-7.

10. Yasuda S, Townsend D, Michele DE, et al. Dystrophic heart failure blocked by membrane sealant poloxamer. Nature 2005;436:1025-9.
11. Yoshimura M, Sakamoto M, Ikemoto M, et al. AAV vector-mediated microdystrophin expression in a relatively small percentage of mdx myofibers improved the mdx phenotype. Mol Ther 2004;10:821-8.
12. Dezawa M, Ishikawa H, Itokazu Y, et al. Bone marrow stromal cells generate muscle cells and repair muscle degeneration. Science 2005;309:314-7.
13. Dell'Agnola C, Wang Z, Storb R, et al. Hematopoietic stem cell transplantation does not restore dystrophin expression in Duchenne muscular dystrophy dogs. Blood 2004;104:4311-8.
14. Wilton SD, Honeyman K, Fletcher S, et al. Snapback SSCP analysis: engineered conformation changes for the rapid typing of known mutations. Hum Mutat 1998;11:252-8.
15. Valentine BA, Cooper BJ, de Lahunta A, et al. Canine X-linked muscular dystrophy. An animal model of Duchenne muscular dystrophy: clinical studies. J Neurol Sci 1988;88:69-81.
16. Kornegay JN, Bogan DJ, Bogan JR, et al. Contraction force generated by tarsal joint flexion and extension in dogs with golden retriever muscular dystrophy. J Neurol Sci 1999;166:115-21.
17. Bartlett RJ, Winand NJ, Secore SL, et al. Mutation segregation and rapid carrier detection of X-linked muscular dystrophy in dogs. Am J Vet Res 1996;57:650-4.
18. Valentine BA, Cooper BJ. Canine X-linked muscular dystrophy: selective involvement of muscles in neonatal dogs. Neuromuscul Disord 1991;1:31-8.
19. Nguyen F, Cherel Y, Guigand L, et al. Muscle lesions associated with dystrophin deficiency in neonatal golden retriever puppies. J Comp Pathol 2002;126:100-8.
20. Seksel K. Puppy socialization classes. Vet Clin North Am Small Anim Pract 1997;27:465-77.
21. Valentine BA, Cooper BJ, Cummings JF, et al. Canine X-linked muscular dystrophy: morphologic lesions. J Neurol Sci 1990;97:1-23.
22. Jaffe KM, McDonald CM, Ingman E, et al. Symptoms of upper gastrointestinal dysfunction in Duchenne muscular dystrophy: case-control study. Arch Phys Med Rehabil 1990;71:742-4.
23. Willig TN, Paulus J, Lacau Saint Guily J, et al. Swallowing problems in neuromuscular disorders. Arch Phys Med Rehabil 1994;75:1175-81.

doi:10.1016/j.ymthe.2004.07.025

ARTICLE

AAV Vector-Mediated Microdystrophin Expression in a Relatively Small Percentage of *mdx* Myofibers Improved the *mdx* Phenotype

Madoka Yoshimura,[1,2] Miki Sakamoto,[1] Madoka Ikemoto,[1] Yasushi Mochizuki,[1] Katsutoshi Yuasa,[1] Yuko Miyagoe-Suzuki,[1] and Shin'ichi Takeda[1,*]

[1]*Department of Molecular Therapy, National Institute of Neuroscience, National Center of Neurology and Psychiatry, 4-1-1 Ogawa-higashi, Kodaira, Tokyo 187-8502, Japan*
[2]*Department of Neurology, Division of Neuroscience, Graduate School of Medicine, University of Tokyo, Hongo 7-3-1, Tokyo 113-8655, Japan*

**To whom correspondence and reprint requests should be addressed. Fax: +81 42 346 1750. E-mail: takeda@ncnp.go.jp.*

Available online 19 August 2004

Duchenne muscular dystrophy (DMD) is a lethal disorder of skeletal muscle caused by mutations in the *dystrophin* gene. Adeno-associated virus (AAV) vector-mediated gene therapy is a promising approach to the disease. Although a rod-truncated microdystrophin gene has been proven to ameliorate dystrophic phenotypes, the level of microdystrophin expression required for effective gene therapy by an AAV vector has not been determined yet. Here, we constructed a recombinant AAV type 2 vector, AAV2-MCKΔCS1, expressing microdystrophin (ΔCS1) under the control of a muscle-specific MCK promoter and injected it into TA muscles of 10-day-old and 5-week-old *mdx* mice. AAV2-MCKΔCS1-mediated gene transfer into 5-week-old *mdx* muscle resulted in extensive and long-term expression of microdystrophin and significantly improved force generation. Interestingly, 10-day-old injected muscle expressed microdystrophin in a limited number of myofibers but showed hypertrophy of microdystrophin-positive muscle fibers and considerable recovery of contractile force. Thus, we concluded that AAV2-MCKΔCS1 could be a powerful tool for gene therapy of DMD.

Key Words: Duchenne muscular dystrophy, gene therapy, adeno-associated virus vector, dystrophin, microdystrophin, skeletal muscle, *mdx* mouse, hypertrophy

INTRODUCTION

Duchenne muscular dystrophy (DMD) is an X-linked, lethal disorder of skeletal muscle caused by mutations in the *dystrophin* gene. There is no effective treatment for the disease at present, although gene therapy could be an attractive approach to the disease.

Several methods of gene transfer have been tried for the treatment of dystrophin-deficient muscular dystrophy: naked plasmid injection [1], full-length dystrophin cDNA transfer via a gutted adenovirus vector [2,3], forced splicing using oligonucleotides [4], and gene repair by a chimeric RNA/DNA oligonucleotide [5]. Among several gene transfer methods, an adeno-associated virus (AAV) vector-mediated gene transfer is one of the most promising approaches to DMD because AAV vectors have been shown to evoke minimal immune responses and mediate long-term transgene expression in skeletal muscle [6–8]. Since the capacity of an AAV vector to incorporate an exogenous gene is limited to 4.9 kb, several groups have attempted to truncate the 14-kb dystrophin cDNA to obtain functional microdystrophins to be inserted into AAV vectors [9–13]. We previously constructed three rod-truncated microdystrophins and generated transgenic *mdx* mice expressing these microdystrophins. Among the three microdystrophins tested, only the 4.9-kb microdystrophin CS1 completely prevented muscle degeneration of dystrophin-deficient *mdx* mice [14]. Based on this result, we generated an AAV vector carrying ΔCS1 microdystrophin cDNA, a modified version of CS1 cDNA, and injected the vectors (designated AAV2-MCKΔCS1) directly into both 10-day-old and 5-week-old *mdx* muscles. In this study, we demonstrate that AAV vector-injected *mdx* muscles showed functional recovery even 24 weeks after treatment. Surprisingly, when introduced into neonatal muscle, microdystrophin expression in a relatively small percentage of

1525-0016/$30.00

doi:10.1016/j.ymthe.2004.07.025

muscle fibers dramatically improved the contractile properties of dystrophic muscle. This improvement in contractile force was thought to be achieved by hypertrophied microdystrophin-positive muscle fibers.

RESULTS

Construction of an AAV-2 Vector Carrying Microdystrophin ΔCS1

We constructed an AAV-2 vector encoding microdystrophin ΔCS1 under the control of a truncated, muscle-specific creatine kinase (MCK) promoter [15]. We designated this recombinant AAV vector AAV2-MCKΔCS1. CS1, which has the N-terminal, actin-binding domain, four rod repeats and three hinges, the cysteine-rich domain, and the C-terminal domain, effectively rescued dystrophic phenotypes when introduced as a transgene [14]. To shorten CS1 cDNA (4.9 kb) further, we deleted the 5′ and 3′ untranslated regions (UTRs) and exons 71–78 (alternative splicing regions of dystrophin mRNA) by PCR techniques. We named the resultant 3.8-kb cDNA ΔCS1 (Fig. 1).

Expression of ΔCS1 Microdystrophin at the Sarcolemma after AAV2-MCKΔCS1-Mediated Gene Transfer into *mdx* Muscle

We injected AAV2-MCKΔCS1 into tibialis anterior (TA) muscles of 10-day-old and 5-week-old dystrophin-deficient *mdx* mice (7.5×10^{10} vector genomes (vg) for neonatal muscle; 2.5×10^{11} vg for young muscle). In a natural course, 10-day-old *mdx* muscle shows no obvious dystrophic changes, while 5-week-old *mdx* muscle shows active cycles of the degeneration–regeneration process. We also analyzed contralateral TA muscles from the treated *mdx* mice and TA muscles from age-matched C57BL/10 (B10) mice as controls. When examined at 8 and 24 weeks after AAV2-MCKΔCS1 injection, ΔCS1 had correctly localized at the sarcolemma (Figs. 2A and 2C). Western blot using a dystrophin antibody showed a band of the expected size (138 kDa) in the AAV vector-injected *mdx* muscles (Fig. 2G). Most of the ΔCS1-positive fibers were peripherally nucleated when AAV2-MCKΔCS1 was injected into 10-day-old *mdx* muscles (Figs. 2A and 2B). In contrast, we observed both centrally and peripherally nucleated fibers when the vectors were injected into 5-week-old *mdx* muscle (Figs. 2C and 2D). The mean percentages of ΔCS1-positive fibers were 22.2 ± 11.4% at 8 weeks and 16.5 ± 7.0% at 24 weeks after injection at 10 days of age (Fig. 2E). When injected at 5 weeks of age, the mean percentages of dystrophin-positive fibers were 39.2 ± 15.8% at 8 weeks and 51.5 ± 17.3% at 24 weeks after vector injection (Fig. 2F). Next, we quantified the amount of ΔCS1 protein by immunoblotting. The amount of microdystrophin protein in the AAV-injected *mdx* muscles at 10 days of age was 12.7 ± 8.4% of that of full-length dystrophin in B10 muscle at 8 weeks (data not shown) and 9.2 ± 1.4% at 24 weeks after injection (Fig. 2G). When we injected AAV2-MCKΔCS1 into 5-week-old *mdx* muscles, the amount was 32.6 ± 8.0% of that of B10 muscle at 8 weeks and 39.8 ± 7.0% at 24 weeks after injection (data not shown).

AAV Vector-Mediated ΔCS1 Expression Ameliorated Dystrophic Phenotypes at 24 Weeks after Injection

When we analyzed *mdx* muscles treated at 10 days of age at 24 weeks after vector injection, only a small percentage of the ΔCS1-positive fibers (12.5 ± 7.8%) had central nuclei compared with untreated *mdx* muscle fibers (Fig. 3A), suggesting the protective function of ΔCS1 against muscle degeneration. In contrast, the percentage of

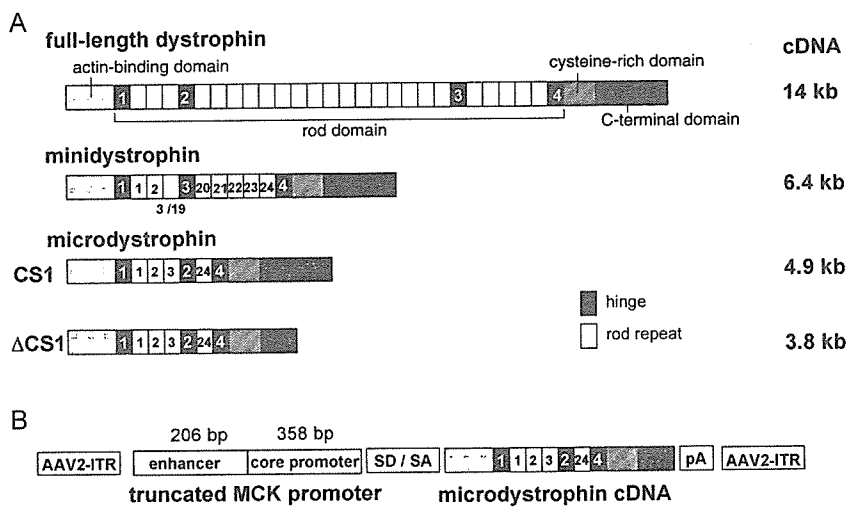

FIG. 1. Diagrams of human full-length dystrophin, minidystrophin, and microdystrophin cDNAs (CS1, ΔCS1) and AAV2-MCKΔCS1. (A) Full-length dystrophin has the N-terminal, actin-binding domain, central rod domain with 24 rod repeats and four hinges, cysteine-rich domain, and C-terminal domain. Minidystrophin, which was cloned from a mild Becker patient and reported previously, is shown as a reference [28]. CS1 has the N-terminal domain, a shortened version of the central rod domain with 4 rod repeats and three hinges, the cysteine-rich domain, and the C-terminal domain [14]. To incorporate microdystrophin CS1 cDNA into the AAV2 vector plasmid, we deleted the 3′ and 5′ untranslated regions and exons 71–78 from CS1 cDNA. The resultant ΔCS1 cDNA is 3.8 kb long. The number of the rod repeats or hinges is shown inside the squares. (B) Structure of the AAV2 vector expressing ΔCS1. ΔCS1 cDNA was incorporated into the AAV2 vector plasmid downstream of the truncated muscle-specific MCK promoter [15].

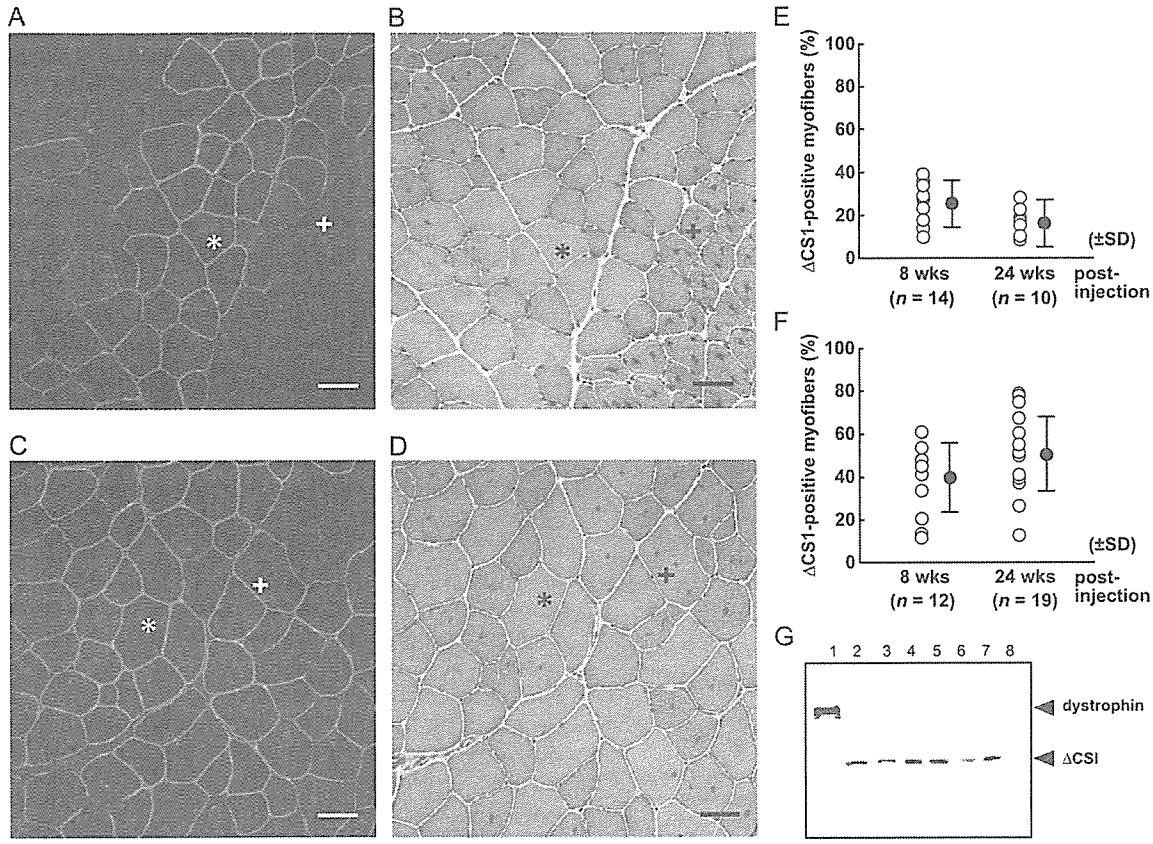

FIG. 2. ΔCS1 expression after AAV vector-mediated gene transfer into skeletal muscles of dystrophin-deficient *mdx* mice. AAV2-MCKΔCS1 was injected into TA muscles of *mdx* mice at (A, B, E) 10 days or at (C, D, F) 5 weeks of age and the muscles were analyzed at 8 or 24 weeks after injection. (A–D) Histological analysis of AAV-injected muscles 24 weeks after AAV injection. Immunofluorescence using a dystrophin antibody (A, C) and H&E staining of serial sections (B, D) is shown. ΔCS1 is correctly localized at the sarcolemma (A, C). Most ΔCS1-positive fibers (*) showed peripherally located nuclei, and their fiber diameters were relatively larger than ΔCS1-negative fibers (+) in the muscles injected at 10 days of age (A, B). In contrast to the muscles injected at the neonatal stage, many centrally nucleated fibers (+) coexist with peripherally nucleated fibers (*) in the muscles injected with the AAV vectors at 5 weeks of age (D). In (A and C), nuclei were stained with TOTO-3 (blue). Bar, 50 μm. (E, F) The percentage of ΔCS1-positive fibers among all fibers of the injected *mdx* muscle. The means (black circles) are indicated ± SD (bars). The percentage of ΔCS1-positive fibers in muscles injected at 5 weeks of age (F) was higher than in the muscles injected at 10 days of age (E). (G) Western blot analysis using a dystrophin antibody of AAV-injected *mdx* muscles. Muscles treated at 10 days of age were analyzed at 24 weeks after injection. Lane 1, C57BL/10 muscle; lanes 2–7, AAV vector-injected *mdx* muscles; lane 8, uninjected *mdx* muscle. Full-length dystrophin (lane 1) and ΔCS1 (lanes 2–7) were detected at the predicted sizes (427 or 138 kDa, respectively).

centrally nucleated fibers among ΔCS1-positive fibers in *mdx* muscles treated at 5 weeks of age (51.5 ± 11.0%) was higher than that of *mdx* muscles treated at 10 days of age (Fig. 3B).

Next, we evaluated the contractile properties of AAV2-MCKΔCS1-injected *mdx* muscle. Untreated *mdx* muscle showed remarkable hypertrophy, but its specific force was much lower than in control B10 muscle (Table 1). Similarly, the wet weight of *mdx* TA muscles treated with AAV2-MCKΔCS1 at 10 days of age was much heavier than that of control B10 TA muscles, but importantly, the maximal force was also increased (Table 1). As a result, there was no statistical difference in specific tetanic force between AAV2-MCKΔCS1-treated *mdx* muscles and age-matched B10 muscles (Table 1).

The transduction efficiency of AAV2 vector-mediated gene transfer into 10-day-old *mdx* mice was relatively low (only up to 20% of positive fibers) (Fig. 2E) compared to gene transfer into 5-week-old *mdx* mice (around 50%) (Fig. 2F), but, surprisingly, the specific tetanic force at 24 weeks after vector injection was almost equivalent to that of age-matched B10 mice and much higher than that of untreated *mdx* muscle (Table 1). To clarify the mechanism of force generation recovery by small percentages of ΔCS1-positive fibers, we next examined the relationship between muscle hypertrophy and force generation. We found a positive correlation ($r = 0.779$, $P < 0.05$) between the wet weight of the AAV2-MCKΔCS1-injected TA muscle and the force generation (Fig. 4A), but not between the muscle weight and the relative interstitial

doi:10.1016/j.ymthe.2004.07.025

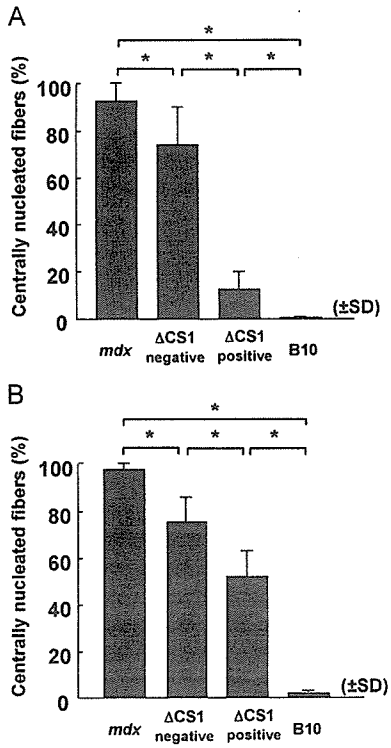

FIG. 3. Microdystrophin ΔCS1 prevents muscle degeneration. Quantitative analysis of centrally nucleated fibers among ΔCS1-positive and -negative fibers in AAV-injected *mdx* muscle. AAV2-MCKΔCS1 was injected into TA muscles of *mdx* mice at (A) 10 days or at (B) 5 weeks of age and analyzed at 24 weeks after injection. Uninjected *mdx* and age-matched control B10 muscles were also examined. (A, B) Most of the ΔCS1-positive fibers in muscles injected at 10 days of age have peripherally located nuclei (A). The percentage of centrally nucleated fibers in ΔCS1-positive fibers in muscles treated at 5 weeks of age (51.5 ± 11.0%) (B) was higher than that in muscles treated at 10 days of age (12.5 ± 7.8%) (A). Note that the ratio of centrally nucleated fibers was significantly reduced even in ΔCS1-negative fibers in muscles injected at both ages. $*P < 0.01$.

area ($r = -0.596$, $P > 0.05$) (Fig. 4B). To confirm whether increased muscle weight reflected myofiber hypertrophy, we measured individual cross-sectional areas (CSAs) of ΔCS1-positive or -negative myofibers in AAV-injected *mdx* muscles. The mean value of fiber CSAs was remarkably larger in ΔCS1-positive *mdx* fibers than in B10 fibers (Fig. 4C). Histogram analysis further demonstrated that the fiber CSA distribution of ΔCS1-positive *mdx* fibers was shifted to the right compared to that of B10 muscle; larger caliber fibers were dominant, reflecting hypertrophy of ΔCS1-expressing fibers (Fig. 4E). Thus, hypertrophied ΔCS1-positive fibers seemed to greatly improve contractile force generation. Some of the untreated and ΔCS1-negative *mdx* fibers were also hypertrophied, but the hypertrophied fibers seemed not to improve the specific force (Fig. 4E).

When we injected 5-week-old mice, force generation was recovered in AAV-injected *mdx* muscles, as when we treated 10-day-old mice, but there was no statistically significant difference in muscle weight between AAV-treated *mdx* muscles and B10 muscles (Table 1). The muscle weight had no correlation with the force generation ($r = -0.512$, $P > 0.05$) (data not shown). In addition, hypertrophy of ΔCS1-positive fibers was not obvious (Fig. 4D). Therefore, we concluded that improved specific force of the *mdx* muscles treated at 5 weeks of age was achieved without hypertrophy, possibly because approximately 50% of the muscle fibers were fully functional for ΔCS1 expression.

DISCUSSION

The level of dystrophin or minidystrophin expression required for effective gene therapy has not been determined yet, although estimates based on either transgenic *mdx* mouse studies [16–18] or the analysis of asymptomatic carriers of dystrophin-deficiency have been reported [19]. Clerk et al. reported that immunostaining showed very few dystrophin-negative fibers in muscles of asymptomatic DMD carriers, while immunoblot analysis revealed a considerable reduction in dystrophin [19]. Furthermore, it was reported that transgenic *mdx* mice expressing a minidystrophin at only 20–30% of endogenous dystrophin levels showed significantly reduced myopathic phenotypes [17]. Phelps et al. suggested that uniform expression of dystrophin is much more beneficial than the variable pattern when the overall levels of dystrophin expression were the same [18]. These findings suggest that the percentage of dystrophin-expressing fibers is more critical than the total amount of the protein. On the other hand, Rafael *et al.* showed that the expression of minidystrophin in only half the *mdx* muscle fibers resulted in a markedly milder phenotype than *mdx* mice showed [16], suggesting that dystrophin-positive fibers rescue surrounding dystrophin-negative fibers from degenerative changes. In this study, we administrated a recombinant AAV vector containing a human microdystrophin gene to the *mdx* muscle and analyzed the relationship between the level or extent of microdystrophin expression and the recovery of contractile force. Importantly, relatively small percentages of muscle fibers (less than 20%) dramatically improved the specific contractile force of dystrophic muscle. Although the molecular mechanisms by which microdystrophin recovers the specific contractile force remain to be shown, this result is encouraging in that the function of dystrophin-deficient muscle might be greatly improved by fewer dystrophin-positive myofibers than previously estimated. As shown in Fig. 3, however, there is a significant reduction in the percentage of centrally nucleated fibers among ΔCS1-negative *mdx* fibers compared to untreated *mdx* muscle, suggesting that microdystrophin expression at levels below the detection limits of immunostaining might be partially protective. There-

TABLE 1: Contractile properties of AAV2-MCKΔCS1-injected *mdx* muscle

	Muscle length (L_0, mm)	Muscle weight (MW, mg)	Maximal force (P_0, mN)	Specific force[a] (mN/mm^2)
		Injection at 10 days of age		
B10 (n = 4)	16.1 ± 0.9	48.7 ± 2.8	91.3 ± 18.1	32.0 ± 5.9
AAV-*mdx* (n = 7)	16.1 ± 1.2	64.3 ± 4.7*,**	116.5 ± 29.9**	30.9 ± 7.9**
mdx (n = 7)	16.1 ± 1.0	70.9 ± 7.0*	79.8 ± 20.0	19.1 ± 3.8*
		Injection at 5 weeks of age		
B10 (n = 6)	15.8 ± 0.9	54.9 ± 5.7	69.0 ± 31.0	20.9 ± 9.0
AAV-*mdx* (n = 11)	15.3 ± 0.8	60.9 ± 6.8	81.7 ± 24.2**	22.3 ± 8.2**
mdx (n = 11)	15.7 ± 0.7	67.9 ± 7.6*	42.2 ± 26.1	10.9 ± 7.5*

Force generation was measured 24 weeks after injection. Data are expressed as means ± SD.

[a] Specific force = ($P_0 \times L_0 \times 1.06$)/MW.

* Significant difference ($P < 0.05$) compared to B10.

** Significant difference ($P < 0.05$) compared to *mdx* muscles.

fore, exact estimation of the percentage of microdystrophin-positive fibers required for the full amelioration is somewhat difficult.

Recovery of absolute maximal force and specific tetanic force is one of the barometers of amelioration. The difference between the contractile properties of ΔCS1-expressing hypertrophied muscle and those of hypertrophied *mdx* muscle by overexpression of IGF-1 [20,21] deserves attention: ΔCS1-positive *mdx* muscle showed considerable recovery of specific force, whereas IGF-mediated hypertrophy modestly restored specific force and the muscle remained susceptible to damage. Similarly, a myostatin blockade of treated *mdx* muscle reportedly improved specific force to some extent, but showed a decrease in ECC force to the same extent as control *mdx* muscle [22]. For comparison of the effects of these different approaches toward DMD therapy, the resistance of ΔCS1-treated muscle to eccentric contraction remains to be evaluated. Importantly, however, myostatin antibody-treated mice showed significantly decreased serum creatine kinase concentrations, suggesting that myostatin blockade endowed dystrophin-deficient fibers with membrane stability.

Positive correlation between muscle wet weight and specific tetanic force indicates that muscle hypertrophy is responsible for functional amelioration at 10-day-old injected *mdx* mice. However, lack of small-caliber, presumably regenerative fibers is the most prominent finding on histograms of ΔCS1-positive *mdx* muscles injected at 10 days of age. Therefore, not only a mild increase in hypertrophic fibers, but also a decrease in small-sized fibers due to inhibition of the cycle of degeneration/regeneration, could greatly contribute to normalization of specific tetanic force. Reduction in embryonic myosin heavy chain and increase in mature myosin heavy chain might contribute to the functional recovery.

Watchko *et al.* injected an AAV2 vector carrying microdystrophin into *mdx* mice and observed incomplete recovery of specific tetanic force with 30–60% of dystrophin-positive fibers [13]. Their microdystrophin was slightly longer than our ΔCS1, it had three hinges, and the C-terminal domain was also deleted. Subtle differences in the construction could affect the functional aspects, and therefore we think that a functional examination of transgenic *mdx* is inevitable.

We also injected AAV2-MCKΔCS1 into 5-week-old *mdx* muscles, which usually show active cycles of muscle degeneration and regeneration. Dystrophin staining revealed that approximately 50% of *mdx* myofibers expressed human-type ΔCS1 microdystrophin 24 weeks after injection. There was no obvious sign of an immune response (data not shown). In contrast to neonatal muscle, *mdx* muscles treated at 5 weeks of age were not hypertrophied but still generated improved contractile force, indicating that widely expressed ΔCS1 could recover muscle function of adult mice without compensatory hypertrophy. Importantly, the CSAs of ΔCS1-positive fibers treated at a neonatal stage were larger than those of ΔCS1-positive fibers treated at 5 weeks of age (Figs. 4C and 4D). One possible explanation for this is that neonatal muscle has a high potency of compensatory hypertrophy in response to force deficit.

Our ΔCS1 and R4-R23/delta71-78, previously reported by Harper et al. [11], have similar structures. R4-R23/delta71-78 robustly transformed centrally nucleated fibers into peripherally nucleated fibers [11]. In contrast, the expression of ΔCS1 in adult *mdx* myofibers resulted in a modest reduction of centrally nucleated fibers when introduced into 5-week-old *mdx* muscle (Fig. 3B). A possible explanation for this discrepancy is a difference in the promoters that drive the microdystrophin expression. Harper *et al.* used a muscle-specific, potent promoter, CK6, and the positions of the Kozak sequences or splicing units are different from ours [11]. These differences might greatly influence the timing and levels of microdystrophin expression. A second possible factor

doi:10.1016/j.ymthe.2004.07.025

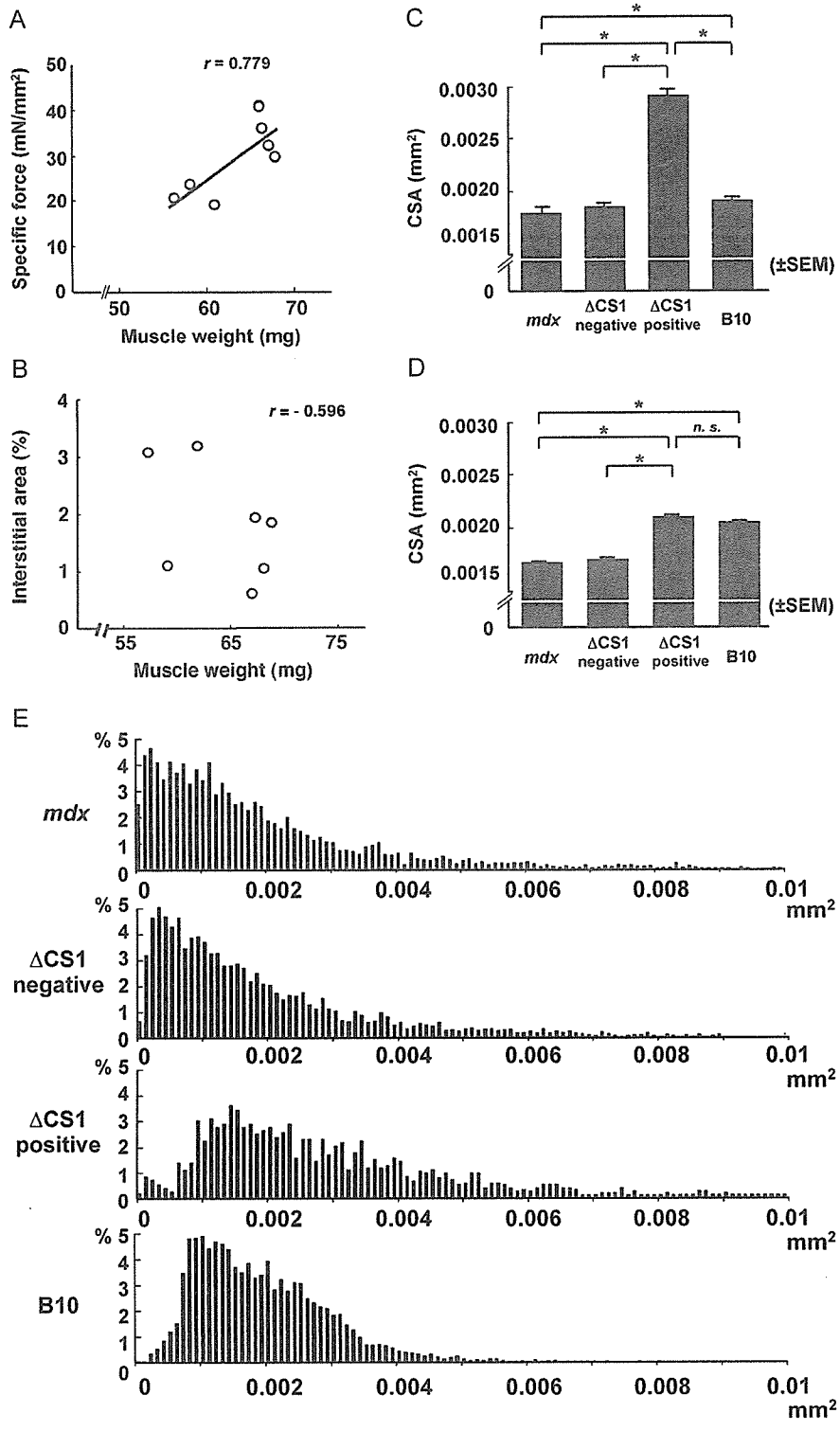

FIG. 4. ΔCS1-positive *mdx* fibers in AAV-treated muscle at 10 days of age show hypertrophy. TA muscles of *mdx* mice were injected with AAV2-MCKΔCS1 at 10 days of age (A–C, E) or at 5 weeks of age (D) and analyzed at 24 weeks after injection. (A) Correlation between muscle wet weight and tetanic force generation ($n = 7$). There was a significant positive correlation between muscle weight and force generation ($r = 0.779$, $P < 0.01$). (B) Relationship between muscle weight and relative interstitial area in AAV-injected muscles ($n = 7$). The increase in muscle weight is not proportional to the interstitial area. (C, D) Mean cross-sectional area (CSA) of uninjected *mdx* muscle fibers and ΔCS1-positive or -negative fibers in AAV-injected *mdx* muscles or age-matched B10 muscle fibers. Three TA muscles were examined for each group. The total numbers of fibers traced were 9674, 6347, 1525, and 5877 in (C) and 8077, 4075, 3479, and 5476 in (D) for *mdx*, ΔCS1-negative *mdx*, ΔCS1-positive *mdx*, and B10 fibers, respectively. When injected at 10 days of age, the CSA of ΔCS1-positive *mdx* fibers was definitely larger than that of normal B10, ΔCS1-negative *mdx*, or contralateral *mdx* fibers (C). In contrast, when mice were treated at 5 weeks of age, the mean CSA of ΔCS1-positive *mdx* fibers was similar to that of B10 muscle and slightly larger than that of *mdx* or ΔCS1-negative *mdx* fibers in treated muscle (D). $^*P < 0.01$. (E) Distribution of the fiber CSAs of untreated *mdx*, ΔCS1-positive, or ΔCS1-negative fibers in *mdx* muscles injected at 10 days of age and age-matched B10 fibers. Shown are the same data set presented in (C). In untreated *mdx* muscles or in ΔCS1-negative *mdx* fibers, small-caliber fibers are dominant, reflecting regeneration. The distribution pattern of ΔCS1-positive fibers deviated to the right, reflecting a larger size than that of B10 fibers. Similar to B10 muscles, small-caliber fibers were markedly reduced in ΔCS1-positive *mdx* fibers, indicating that ΔCS1 prevented muscle degeneration.

is the difference in muscle types used. Harper *et al.* injected AAV vectors into gastrocnemius muscles of 32-day-old mice. The gastrocnemius shows less centrally nucleated fibers than TA muscle in the natural course of the disease (Yuasa *et al.*, unpublished data). In our result, however, AAV-treated *mdx* muscle with a high

percentage of centrally nucleated fibers (50%) did not show dystrophic dysfunction, e.g., decreased force generation. Therefore, centrally nucleated fibers do not disprove the protective function of ΔCS1. The percentage of centrally nucleated fibers would reflect the state of muscles at the time of injection. Our results are important because it is sometimes difficult to start gene therapies before the onset of the clinical course of DMD, and AAV2-MCKΔCS1 is expected to show therapeutic effects even after the onset of disease.

Although we injected high titers of AAV-vector particles into the muscle, the transduction efficiency in 10-day-old *mdx* muscles was much lower than that in 5-week-old *mdx* muscle. This phenomenon was also noticed for the injection of AAV2-CMVLacZ into neonatal B10 muscle (unpublished results). This difference might be due to the preferential expression of receptors or coreceptors for an AAV-2 particle on adult muscle fibers. Several molecules, such as heparan sulfate proteoglycan [23], αVβ5 integrin [24], and dynamin I [25], are proposed to play certain roles in AAV type 2 infection, although the expression of these molecules in muscle fibers during development and aging has not been fully determined. Another possibility is dilution of AAV vectors by rapid growth of neonatal muscle. When we cultured satellite cells prepared from AAV2-CMVLacZ-injected *mdx* muscle, we observed no blue myoblasts or myotubes (data not shown). Therefore, proliferation and fusion of nontransduced satellite cells/myoblasts would greatly dilute the microdystrophin protein.

Our results are promising because AAV vector-mediated ΔCS1 gene transfer had a restorative function for dystrophin-deficient *mdx* muscle. However, demonstration of the benefits of this gene transfer strategy for human DMD patients requires careful testing. Differences between humans and mice, such as muscle size, life span, or biological properties (especially immune responses), should be taken into consideration. A bigger animal model, e.g., canine X-linked muscular dystrophy [26], will contribute to the preclinical study of gene therapy.

MATERIALS AND METHODS

Constructs of human rod-truncated microdystrophin cDNAs and generation of AAV vectors expressing microdystrophin. To incorporate microdystrophin CS1 cDNA (4.9 kb) [14] into an AAV type 2 vector, we further deleted the 3′ and 5′ UTRs and exons 71–78 from CS1 cDNA. In brief, DNA fragments of the 5′-terminal and 3′-terminal regions were independently amplified by PCR to remove exons 71–78 and the 5′ and the 3′ UTRs and then replace them with corresponding sequences of CS1 cDNA. The resulting microdystrophin cDNA was 3.8 kb long and designated ΔCS1. Microdystrophin ΔCS1 cDNA was then cloned into an AAV type 2 vector plasmid [15]. The recombinant AAV vector expressing ΔCS1 under the control of the truncated muscle-specific MCK promoter, designated AAV2-MCKΔCS1, was then purified and titrated as previously described [15].

Administration of AAV vector to murine skeletal muscle. Fifteen microliters (7.5×10^{10} vg) or 50 μl (2.5×10^{11} vg) of AAV2-MCKΔCS1 was injected directly into the right TA muscles of dystrophin-deficient C57BL/10 *mdx* mice at 10 days or 5 weeks of age, respectively. AAV vector-injected and uninjected *mdx* muscles and normal muscles of age-matched C57BL/10 mice were isolated at 8 and 24 weeks after injection.

Contractile properties of AAV2-MCKΔCS1-injected TA muscles. Tetanic force generation was measured and analyzed as described previously with some modifications [14,27]. The entire TA muscle was removed with its tibial origin intact, and the distal portion of the TA tendon and its origin was secured with a 5-O silk suture. The TA was mounted in a vertical tissue chamber and connected to a force transducer, UL-10GR (Minerva, Nagano, Japan), and a length servosystem, MM-3 (Narishige, Tokyo, Japan). Electrical stimulation using a SEN3301 (Nihon Kohden, Tokyo, Japan) was applied through a pair of platinum wires placed on both sides of the muscle in physiological soft solution (150 mM NaCl, 4 mM KCl, 2 mM $CaCl_2$, 1 mM $MgCl_2$, 5.6 mM glucose, 5 mM Hepes, pH 7.4, and 0.02 mM D-tubocurarine). Muscle fiber length was adjusted incrementally by using a micropositioner until peak isometric twitch force responses were obtained (optimal fiber length (L_0)). Maximal tetanic force (P_0) was assessed by stimulation frequencies of 125 pulses/s delivered in 500-ms duration trains with 2 min intervening between each train. Following two measurements, the stimulated muscle was weighed after tendon and bone attachments were removed. All forces were normalized to the physiological cross-sectional area (pCSA), the latter estimated on the basis of the following formula: muscle wet weight (in mg)/(L_0 (in mm) × 1.06 (in mg/mm^3)). The estimated pCSA was used to determine specific tetanic force (P_0/pCSA) of the muscle. After measurement of contractile force, the muscle was quickly frozen in liquid nitrogen-cooled isopentane for histopathological analysis.

Histopathological analyses. Histological, immunohistochemical, and Western blot analyses were performed as described [14]. After blocking with an M.O.M. kit (Vector Laboratories, Burlingame, CA, USA), dystrophin was detected using a monoclonal anti-dystrophin antibody NCL-DysB (Novocastra, Newcastle, UK; 1:20 dilution) and visualized with Alexa 488-labeled goat anti-mouse IgG antibody (Molecular Probes, Eugene, OR, USA) (1:200 dilution). Nuclei were stained with TOTO-3 (Molecular Probes). In some cases, the signal was visualized with diaminobenzidine and counterstained with hematoxylin. We counted the number of centrally or peripherally nucleated fibers in dystrophin-positive or -negative fibers of whole cross sections of TA muscle. In addition, the CSA of each fiber was measured using an image analysis system, ImagePro-Plus (Media Cybernetics, Silver Spring, MD, USA). To evaluate the level of fibrosis, we performed modified Masson trichrome staining, and the blue-stained area was measured using Image Pro-Plus. The relative connective tissue area was calculated to the entire muscle cross-sectional area (%). The signals on immunoblotting were quantitated using NIH Image.

Statistical analysis. Data were expressed as means ± SD or ± SEM. If a significant F ratio was detected by analysis of variance, comparisons among each group were performed using Fisher's PLSD. A P value of <0.05 or <0.01 was considered statistically significant. The relation between the muscle weight and the specific tetanic force was analyzed with Pearson's correlation coefficient ($P < 0.05$).

ACKNOWLEDGMENTS

We are greatly appreciative of Ryoko Nakagawa and Satoru Masuda for their technical support. We thank Ayako Sakamoto, Kunimasa Arima (Department of Laboratory Medicine, National Center Hospital for Mental, Nervous and Muscular Disorders), and Michiko Sagishima (Department of Pathology, School of Medicine, Teikyo University) for advising on pathological techniques. This work is supported by Grants-in-Aid from the Center of Excellence, Research on Nervous and Mental Disorders (10B-1, 13B-1), and Health Sciences Research Grants for Research on the Human Genome and Gene Therapy (H10-genome-015, H13-genome-001) from the Ministry of Health, Labor, and Welfare of

doi:10.1016/j.ymthe.2004.07.025

Japan, and a Grant-in-Aid for Scientific Research (B) from the Ministry of Education, Science, Sports, and Culture of Japan.

RECEIVED FOR PUBLICATION FEBRUARY 28, 2004; ACCEPTED JULY 20, 2004.

REFERENCES

1. Acsadi, G., *et al.* (1991). Human dystrophin expression in *mdx* mice after intramuscular injection of DNA constructs. *Nature* **29:** 815–818.
2. Gilbert, R., *et al.* (2001). Dystrophin expression in muscle following gene transfer with a fully deleted ("gutted") adenovirus is markedly improved by trans-acting adenoviral gene products. *Hum. Gene Ther.* **20:** 1741–1755.
3. DelloRusso, C., *et al.* (2002). Functional correction of adult *mdx* mouse muscle using gutted adenoviral vectors expressing full-length dystrophin. *Proc. Natl. Acad. Sci. USA* **99:** 12979–12984.
4. Lu, Q. L., *et al.* (2003). Functional amounts of dystrophin produced by skipping the mutated exon in the *mdx* dystrophic mouse. *Nat. Med.* **9:** 1009–1014.
5. Bartlett, R. J., *et al.* (2000). In vivo targeted repair of a point mutation in the canine dystrophin gene by a chimeric RNA/DNA oligonucleotide. *Nat. Biotechnol.* **18:** 615–622.
6. Xiao, X., Li, J., and Samulski, R. J. (1996). Efficient long-term gene transfer into muscle tissue of immunocompetent mice by adeno-associated virus vector. *J. Virol.* **70:** 8098–8108.
7. Kessler, P. D., *et al.* (1996). Gene delivery to skeletal muscle results in sustained expression and systemic delivery of a therapeutic protein. *Proc. Natl. Acad. Sci. USA* **26:** 14082–14087.
8. Fisher, K. J., *et al.* (1997). Recombinant adeno-associated virus for muscle directed gene therapy. *Nat. Med.* **3:** 306–312.
9. Yuasa, K., *et al.* (1998). Effective restoration of dystrophin-associated proteins in vivo by adenovirus-mediated transfer of truncated dystrophin cDNAs. *FEBS Lett.* **27:** 329–336.
10. Wang, B., Li, J., and Xiao, X. (2000). Adeno-associated virus vector carrying human minidystrophin genes effectively ameliorates muscular dystrophy in *mdx* mouse model. *Proc. Natl. Acad. Sci. USA* **5:** 13714–13719.
11. Harper, S. Q., *et al.* (2002). Modular flexibility of dystrophin: implications for gene therapy of Duchenne muscular dystrophy. *Nat. Med.* **8:** 253–261.
12. Fabb, S. A., Wells, D. J., Serpente, P., and Dickson, G. (2002). Adeno-associated virus vector gene transfer and sarcolemmal expression of a 144 kDa micro-dystrophin effectively restores the dystrophin-associated protein complex and inhibits myofibre degeneration in nude/*mdx* mice. *Hum. Mol. Genet.* **1:** 733–741.
13. Watchko, J., *et al.* (2002). Adeno-associated virus vector-mediated minidystrophin gene therapy improves dystrophic muscle contractile function in *mdx* mice. *Hum. Gene Ther.* **10:** 1451–1460.
14. Sakamoto, M., *et al.* (2002). Micro-dystrophin cDNA ameliorates dystrophic phenotypes when introduced into *mdx* mice as a transgene. *Biochem. Biophys. Res. Commun.* **17:** 1265–1272.
15. Yuasa, K., *et al.* (2002). Adeno-associated virus vector-mediated gene transfer into dystrophin-deficient skeletal muscles evokes enhanced immune response against the transgene product. *Gene Ther.* **9:** 1576–1588.
16. Rafael, J., *et al.* (1994). Prevention of dystrophic pathology in *mdx* mice by a truncated dystrophin isoform. *Hum. Mol. Genet.* **3:** 1725–1733.
17. Wells, D., *et al.* (1995). Expression of human full-length and minidystrophin in transgenic *mdx* mice: implications for gene therapy of Duchenne muscular dystrophy. *Hum. Mol. Genet.* **4:** 1245–1250.
18. Phelps, S. F., *et al.* (1995). Expression of full-length and truncated dystrophin minigenes in transgenic *mdx* mice. *Hum. Mol. Genet.* **4:** 1251–1258.
19. Clerk, A., et al. (1991). Characterisation of dystrophin in carriers of Duchenne muscular dystrophy. *J. Neurol. Sci.* **102:** 197–205.
20. Gregorevic, P., Plant, D. R., Leeding, K. S., Bach, L. A., and Lynch, G. S. (2002). Improved contractile function of the *mdx* dystrophic mouse diaphragm muscle after insulin-like growth factor-I administration. *Am. J. Pathol.* **161:** 2263–2272.
21. Barton, E. R., Morris, L., Musaro, A., Rosenthal, N., and Sweeney, H. L. (2002). Muscle-specific expression of insulin-like growth factor I counters muscle decline in *mdx* mice. *J. Cell Biol.* **157:** 137–148.
22. Bogdanovich, S., et al. (2002). Functional improvement of dystrophic muscle by myostatin blockade. *Nature* **28:** 418–421.
23. Summerford, C., and Samulski, R. J. (1998). Membrane-associated heparan sulfate proteoglycan is a receptor for adeno-associated virus type 2 virions. *J. Virol.* **72:** 1438–1445.
24. Summerford, C., Bartlett, J. S., and Samulski, R. J. (1999). AlphaVbeta5 integrin: a co-receptor for adeno-associated virus type 2 infection. *Nat. Med.* **5:** 78–82.
25. Duan, D., *et al.* (1999). Dynamin is required for recombinant adeno-associated virus type 2 infection. *J. Virol.* **73:** 10371–10376.
26. Shimatsu, Y., *et al.* (2003). Canine X-linked muscular dystrophy in Japan (CXMDj). *Exp. Anim.* **52:** 93–97.
27. Hosaka, Y., *et al.* (2002). Alpha1-syntrophin-deficient skeletal muscle exhibits hypertrophy and aberrant formation of neuromuscular junctions during regeneration. *J. Cell Biol.* **16:** 1097–1107.
28. England, S. B., *et al.* (1990). Very mild muscular dystrophy associated with the deletion of 46% of dystrophin. *Nature* **343:** 180–182.

Available online at www.sciencedirect.com
SCIENCE DIRECT®
Biochemical and Biophysical Research Communications 321 (2004) 1050–1061
BBRC
www.elsevier.com/locate/ybbrc

Mac-1^{low} early myeloid cells in the bone marrow-derived SP fraction migrate into injured skeletal muscle and participate in muscle regeneration ☆

Koichi Ojima [a,b], Akiyoshi Uezumi [a], Hiroyuki Miyoshi [c], Satoru Masuda [a], Yohei Morita [d,e], Akiko Fukase [a], Akihito Hattori [b], Hiromitsu Nakauchi [d,e], Yuko Miyagoe-Suzuki [a], Shin'ichi Takeda [a,*]

[a] *Department of Molecular Therapy, National Institute of Neuroscience, National Center of Neurology and Psychiatry, 4-1-1 Ogawa-higashi, Kodaira, Tokyo 187-8502, Japan*
[b] *Department of Animal Science, Faculty of Agriculture, Hokkaido University, Kita 9, Nishi 9, Kita-ku, Sapporo, Hokkaido 060-8589, Japan*
[c] *BioResource Center, RIKEN Tsukuba Institute, 3-1-1 Koyadai, Tsukuba, Ibaraki 305-0074, Japan*
[d] *Laboratory of Stem Cell Therapy, Center for Experimental Medicine, The Institute of Medical Science, The University of Tokyo, 4-6-1 Shirokanedai, Minato-ku, Tokyo 108-8639, Japan*
[e] *Department of Immunology, Institute of Basic Medical Sciences, The University of Tsukuba, and CREST (JST), 1-1-1 Tennodai, Tsukuba, Ibaraki 305-8575, Japan*

Received 20 May 2004

Abstract

Recent studies have shown that bone marrow (BM) cells, including the BM side population (BM-SP) cells that enrich hematopoietic stem cells (HSCs), are incorporated into skeletal muscle during regeneration, but it is not clear how and what kinds of BM cells contribute to muscle fiber regeneration. We found that a large number of SP cells migrated from BM to muscles following injury in BM-transplanted mice. These BM-derived SP cells in regenerating muscles expressed different surface markers from those of HSCs and could not reconstitute the mouse blood system. BM-derived SP/Mac-1^{low} cells increased in number in regenerating muscles following injury. Importantly, our co-culture studies with activated satellite cells revealed that this fraction carried significant potential for myogenic differentiation. By contrast, mature inflammatory (Mac-1^{high}) cells showed negligible myogenic activities. Further, these BM-derived SP/Mac-1^{low} cells gave rise to mononucleate myocytes, indicating that their myogenesis was not caused by stochastic fusion with host myogenic cells, although they required cell-to-cell contact with myogenic cells for muscle differentiation. Taken together, our data suggest that neither HSCs nor mature inflammatory cells, but Mac-1^{low} early myeloid cells in the BM-derived SP fraction, play an important role in regenerating skeletal muscles.

Keywords: Side population cells; Muscle regeneration; Myogenic differentiation; Bone marrow; Muscular dystrophy

Skeletal muscles have a remarkable capacity for regeneration in response to various types of damage, such as chemicals, stretching, exercise, injury, and diseases including inherited muscular dystrophies. Satellite cells are skeletal muscle-specific precursors and play an important role in muscle fiber regeneration [3]. They are located beneath the basement membrane and are mitotically

☆ *Abbreviations:* β-Gal, β-galactosidase; BM, bone marrow; CTX, cardiotoxin; FACS, fluorescence-activated cell sorting; GC, gastrocnemius; GFP, green fluorescence protein; HE, hematoxylin and eosin; HSC, hematopoietic stem cell; MP, main population; SP, side population; TA, tibialis anterior; X-Gal, 5-bromo-4-chloro-3-indolyl β-D-galactopyranoside.

* Corresponding author. Fax: +81 42 346 1750.
E-mail address: takeda@ncnp.go.jp (S. Takeda).

0006-291X/$ - see front matter © 2004 Elsevier Inc. All rights reserved.
doi:10.1016/j.bbrc.2004.07.069

quiescent in adult muscle. Once muscle is damaged, they are activated, proliferate enormously, and fuse with each other or with pre-existing muscle fibers to produce fully mature muscle fibers [3,33]. They have been considered the only cells that give rise to myoblasts and form new myofibers in adult skeletal muscle [3,38].

Recently, cells with myogenic potential have been found in non-muscle tissues. They are involved in bone marrow (BM) [4–6,8,12,13,15,18,22,35], dorsal aorta [10], fetal liver [15], synovial membrane [11], and epidermis [24]. Among them, BM is an attractive source tissue for cell-based therapy for muscular dystrophy because it is thought that BM cells with myogenic potential are disseminated to all muscles in the body through the circulation. More recently, LaBarge and Blau [22] demonstrated that transplanted BM cells were progressively recruited as satellite cells and that subsequent exercise induced them to participate in muscle regeneration, suggesting that donor-derived BM cells contribute to muscle fibers in a step-wise biological progression.

Furthermore, it has been reported that BM side population (BM-SP) cells, which efficiently efflux Hoechst dye 33342 and enrich hematopoietic stem cells (HSCs) [16,17], participated in skeletal muscle regeneration in lethally irradiated mice [7,18]. Recently, Camargo et al. [6] and Corbel et al. [8] have reported that a single BM-SP cell was able to both reconstitute the hematopoietic system and contribute to muscle regeneration. Although Camargo et al. [6] suggested that cells committed to the myeloid lineage were incorporated into newly forming myofibers, it is still unclear what types of myeloid cells preferentially contribute to regenerating myofibers.

Several BM transplantation studies [4,6,8,12,15, 18,22] indicate that donor-derived myofibers are frequently detected in regenerated fibers or in exercised muscles, although they are quite rare in normal conditions. This phenomenon is possibly related to increased recruitment of BM-derived myogenic progenitor cells or stem cells into damaged muscle via the blood stream. In addition, it is likely that cytokines released in inflamed muscles direct the myogenic commitment of BM cells.

Here we demonstrated that a large number of SP cells migrated from BM to regenerating muscles, where the BM-derived SP cells did not have hematopoietic potential but did directly participate in muscle regeneration. Further, we showed that cells with myogenic potential were enriched in BM-derived SP cells with low expression of Mac-1 antigen in regenerating muscles. These findings further support the potential of BM-SP cell-based therapy for dystrophic muscular disorders.

Materials and methods

Experimental animals. All procedures used on experimental animals were approved by the Experimental Animal Care and Use Committee at the National Institute of Neuroscience. C57BL/6 mice were purchased from Nihon CLEA (Tokyo, Japan). C57BL/6-*GFP*-transgenic mice were kindly provided by Dr. Okabe (Osaka University, Japan). C57BL/6-Rosa26 mice were obtained from the Jackson Laboratory (Bar Harbor, ME).

Preparation of BM and BM-SP cells. Bone marrow cells were sterilely isolated from the femurs and tibias of *GFP* transgenic mice [27]. Marrow fragments were filtered through 40 μm nitrex mesh (BD Bioscience, Franklin Lakes, NJ) and subsequently through 10 μm nylon mesh (Kyoshin Rikoh, Tokyo, Japan). After removing red blood cells with Lympholyte-M (Cedarlane, Hornby, Ontario), BM cells were used for BM cell-transplantation or isolation of SP cells.

The BM-SP fraction was prepared as described by Goodell et al. (http://www.bcm.tmc.edu/genetherapy/goodell/newsite/protocols.html). BM cells were re-suspended at 10^6 cells/ml in Dulbecco's modified Eagle's medium (DMEM) (Invitrogen, Carlsbad, CA) containing 2% fetal bovine serum (FBS) (Trace Biosciences, New South Wales, Australia), 10 mM Hepes, and 5 μg/ml Hoechst 33342 (Sigma Chemical, St. Louis, MO) and incubated for 90 min at 37 °C in the presence or the absence of 50 μM Verapamil (Sigma). For antibody staining, cells were incubated on ice for 30 min in the presence of a 1:100 dilution of PE- or APC-conjugated anti-CD45 antibody, PE-conjugated anti-CD11b/CD18 (Mac-1) antibody, PE-conjugated Sca-1 antibody, biotin-conjugated anti-CD34 antibody, or biotin-conjugated anti-c-kit antibody (BD PharMingen, San Diego, CA). For biotin-conjugated antibodies, 1:100 diluted PE- or APC-conjugated streptavidin (BD PharMingen) was further labeled for 15 min on ice. After washing, stained cells were re-suspended in PBS containing 2% FBS and 2 μg/ml propidium iodide (PI) (BD PharMingen). Cell sorting was performed on a FACS VantageSE flow cytometer (Falcon, Franklin Lakes, NJ). Hoechst staining and subsequent antibody labeling indicated a viability of 84.2 ± 11.5% (means ± SD, $n = 18$) as expressed by the percentage of total PI-negative cells per total cells. The BM-SP accounted for 0.026 ± 0.017% (means ± SD, $n = 18$) of viable unfractionated BM without red blood cells. Debris and dead cells were excluded by forward scatter, side scatter, and PI gating. We used only PI-negative fractions for further experiments.

Preparation of mononucleated cells from muscle. Cardiotoxin (CTX) (Wako Pure Chemical Industries, Tokyo, Japan) -injected and uninjected skeletal muscles were dissected from GFP^+BM-SP/$CD45^+$ cell-transplanted mice and the *GFP* transgenic mice. We carefully removed nerves, blood vessels, tendons, and fat tissues from muscles under a dissection microscope. Trimmed muscles were minced and then treated with 0.2% type II collagenase (Worthington Biochemical, Lakewood, NJ) for 40 min at 37 °C [20]. Muscle slurries were filtered through 100 μm nitrex mesh (BD Bioscience) and subsequently through 40 μm nitrex mesh (BD Bioscience). Erythrocytes were eliminated by treatment with 0.8% NH_4Cl in Tris-buffer solution. Mononucleated cells were stained with Hoechst 33342 and antibodies as described in BM-SP staining. Then stained cells were analyzed with a FACS VantageSE flow cytometer (Falcon). Hoechst staining and subsequent antibody labeling indicated a viability of 87.5 ± 1.3% (means ± SD, $n = 3$) and 68.5 ± 3.2% (means ± SD, $n = 3$) expressed as the percentage of total PI-negative cells per total mononucleated cells from injured muscles and uninjured muscles, respectively. The SP cells accounted for 0.81 ± 0.25% (means ± SD, $n = 9$) and 1.72 ± 0.13% (means ± SD, $n = 3$) of viable unfractionated mononucleate cells without red blood cells from injured muscles and uninjured muscles, respectively. We used only PI-negative fractions for further experiments.

Transplantation experiments. After X-irradiation with 5 or 9 Gy (Hitachi Medical, Tokyo, Japan), 5×10^6–1×10^7 unfractionated GFP^+ BM cells, 2000 GFP^+ BM-SP/$CD45^+$ cells, or 3000 GFP^+ SP/$CD45^+$ cells from regenerating muscles of *GFP* transgenic mice were transplanted retroorbitally into 8- to 10-week-old C57BL/6 mice. For transplantation of GFP^+ SP/$CD45^+$ cells from BM and GFP^+ SP/$CD45^+$ cells from regenerating muscles, 2×10^5 unfractionated BM cells from C57BL/6 mice were also transplanted as competitor cells. SP

cells were isolated from PI-negative fractions and immediately used for transplantation assay. GFP chimerism was calculated by the ratio of GFP^+ cells to total mononucleated cells in BM or peripheral blood. Twelve to 15 weeks after transplantation, transplanted mice were subjected to CTX injection studies and FACS analysis.

Cardiotoxin injection and tissue preparation. To induce muscle regeneration, 0.1 ml of 10 μM CTX was injected into the TA and/or GC muscles of transplanted mice with a 27-gauge needle [9,14,19]. The CTX-injected TA and/or GC muscles and the non-injected contralateral TA and/or GC muscles were dissected for histological analysis at 3–4 weeks or 8–10 weeks after CTX injection. Following fixation with 4% paraformaldehyde in PBS for 30 min, muscles were sequentially soaked in 10% sucrose in PBS and 20% sucrose in PBS. For histological and immunohistochemical analysis, muscles were frozen in isopentane cooled with liquid nitrogen.

Histological and immunohistochemical analysis. Muscle cryostat sections (7 μm) were stained with hematoxylin and eosin (HE). Serial cross-sections were blocked with 5% goat serum in PBS and then reacted with anti-GFP antibody (1:100; Chemicon International, Temecula, CA), anti-laminin α2 antibody (1:100; clone 4H8-2; Alexis, San Diego, CA), anti-CD11b/18 (Mac-1) antibody (1:100; Cedarlane), and/or anti-M-cadherin antibody (1:10,000) at 4 °C overnight. Anti-M-cadherin antibody was generated by fusing the mouse M-cadherin cDNA sequence corresponding to 339–444 aa to GST in a pGEX vector (Amersham Biosciences, Piscataway, NJ), and the GST-M-cadherin fusion protein was used as an antigen. The rabbit anti-serum obtained was affinity purified. The sections were incubated with appropriate combinations of Alexa 488-, Alexa 568-, and Alexa 594-labeled secondary antibodies (Molecular Probes, Eugene, OR) for 30 min. Nuclei were stained with TOTO3 (Molecular Probes). Stained sections were observed under a confocal laser scanning microscope (Leica TCS SP; Leica, Heidelberg, Germany).

Preparation of activated satellite cells. Single myofibers were prepared as described in the literature [2,31] with slight modifications. In brief, dissected extensor digitorum longus (EDL) muscles from C57BL/6 mice or C57BL/6-Rosa26 mice were digested with 0.5% type I collagenase (Worthington Biochemical) at 37 °C for 90 min. Five to ten intact, viable single myofibers were plated on chamber slides (Nalge Nunc International, Naperville, IL) coated with Matrigel (Collaborative Biomedical Products, Bedford, MA), and cultured with DMEM (Invitrogen) containing 10% horse serum (HS) (BioWhittaker, Walkersville, MD) and 0.5% chick embryo extract (CEE) (Invitrogen) in a humid 5% CO_2 environment at 37 °C for 4 days. To proliferate mononucleated myogenic cells, they were kept in growth medium (10% HS, 20% FBS, and 1% CEE in DMEM).

For immunostaining, cultured cells were fixed with 2% formaldehyde in PBS for 10 min. After washing with 0.5% Triton X-100 in PBS, specimens were blocked with 5% goat serum (Cedarlane) in PBS for 15 min, then incubated with anti-GFP antibody (1:500; Chemicon) and anti-sarcomeric α-actinin antibody (1:1000; Sigma) for 1 h at 37 °C, and then reacted with secondary antibody conjugated with Alexa 488 or Alexa 568 (Molecular Probes). Nuclei were detected with Hoechst 33258 (Molecular Probes). To detect β-galactosidase activity, cells were stained with 5-bromo-4-chloro-3-indolyl β-D-galactopyranoside (X-Gal).

Co-culture of BM-derived SP cells with activated satellite cells. After approximately 7 days culture, myofiber-derived activated satellite cells reached 50–70% confluence. At this point, co-culture with BM-SP cells was started. Approximately 500–2500 freshly isolated GFP^+ BM-SP/$CD45^+$ cells were added to 3000–5000 activated satellite cells derived from C57BL/6 myofibers. Differentiation medium (10% HS, 2% FBS, and 0.5% CEE in DMEM) was applied soon after starting co-culture. Approximately 4000–5000 SP/$CD45^+$ cells, 4000–5000 SP/$CD45^+$ Mac-1^- cells, 2000 SP/$CD45^+$ Mac-1^{low} cells, 10,000 main population (MP)/$CD45^+$ cells, 10,000 MP/$CD45^+$ Mac-1^{low} cells, or 10,000 MP/$CD45^+$ Mac-1^+ cells from *GFP* transgenic mouse muscles damaged by CTX injection were co-cultured with 10,000 activated satellite cells from C57BL/6 mice. For BM-derived SP cells from regenerating muscles, cells were kept in growth medium (20% FBS, 2.5 ng/ml basic fibroblast growth factor (Pepro Tech EC, London, England) in DMEM) for 4 days and then switched to differentiation medium for further culture. Less than 20% of plated BM-SP cells survived 2 days after starting co-culture. Approximately 5–10% plated BM-derived cells from regenerating muscles survived 2 days after starting co-culture. Cultured cells were observed with phase-contrast and fluorescence microscopy IX70 (OLYMPUS, Tokyo, Japan).

Results

Contribution of BM-SP cells to muscle fibers in vivo

To investigate which type of donor cells contributes to muscle fibers, unfractionated BM cells or BM-SP cells from *GFP* transgenic mice [27] were transplanted into X-irradiated C57BL/6 mice. To further compare the efficiency of myogenic contributions of donor-derived cells to damaged muscles or intact muscles, we injected cardiotoxin (CTX) into tibialis anterior (TA) and/or gastrocnemius (GC) muscles more than 12 weeks after transplantations to induce muscle regeneration. For BM-SP cell transplantation, we selected the $CD45^+$ fraction of BM-SP cells (BM-SP/$CD45^+$) to exclude the possible contamination of mesenchymal stem cells [34]. The frequency of donor-derived GFP^+ fibers in damaged muscle was relatively higher than in undamaged muscle (Fig. 1, Table 1). The ratio of GFP^+ myofibers normalized to the number of transplanted cells was significantly higher in BM-SP/$CD45^+$ cell-transplanted mice than in unfractionated BM cell-transplanted mice (Table 1). Contrary to previous reports [15,22], we have not detected donor-derived GFP^+ satellite cells in muscle sections and in cultures of isolated single myofibers from transplanted mice (data not shown).

Migration of SP cells from BM to regenerating muscle

CTX injection experiments suggested that muscle damage enhanced the contribution of BM-SP/$CD45^+$ cells to muscle fiber formation and that muscle injuries could increase the migration of BM cells with myogenic potential to the injury site via the bloodstream. Therefore, we examined whether SP cells migrate or not from BM to regenerating muscle by the use of GFP^+ BM-SP/$CD45^+$ cell-transplanted mice. Twelve to 15 weeks after transplantation, CTX was injected into TA muscles. Three days after the injury, a considerable number of donor-derived GFP^+ cells were found in damaged muscles (Figs. 2A–D). At this early stage of muscle regeneration, M-cadherin immunostaining revealed many activated satellite cells proliferating inside the pre-existing basement membrane sheath (Fig. 2E).

Next, we isolated mononucleated cells from intact or damaged muscles and analyzed them by fluorescence-activated cell sorting (FACS). SP cells, which are sensitive to Verapamil, were involved in both intact and damaged

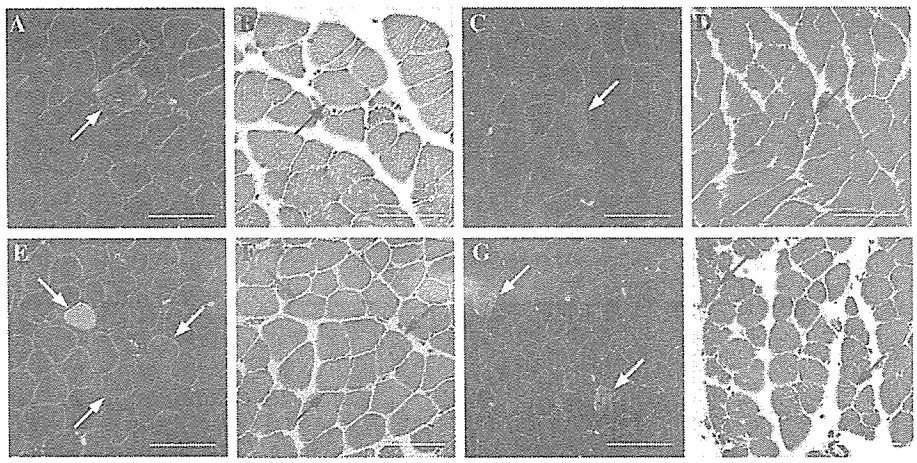

Fig. 1. Contribution of transplanted BM cells to myofibers in mice. (A–H) Unfractionated GFP$^+$ BM cells (A,B,E, and F) or GFP$^+$ BM-SP/CD45$^+$ cells (C,D,G, and H) were transplanted into lethally X-irradiated C57BL/6 mice. Twelve to 15 weeks after transplantation, CTX was injected into TA and/or GC muscles to induce muscle regeneration (E–H). Undamaged muscles are shown in (A–D). At 10 weeks after CTX injection, cryostat sections of TA (A,B,E,F,G, and H) and GC (C,D) muscles were stained with anti-GFP antibody (green in A,C,E, and G) and anti-laminin α2 antibody (red in A,C,E, and G). HE-stained sections (B,D,F, and H) are serial sections of (A,C,E, and G), respectively. Arrows indicate GFP-positive myofibers. Bars, 80 μm.

Table 1
Quantitation of donor-derived myofibers in transplanted mice

Mouse ID No.	X-ray (Gy)	Transplanted cell	GFP-chimerism in BM (%)	Muscle	CTX[a]	GFP$^+$ myofibers	Total myofibers	%[b]	%[c]
52	9	GFP$^+$ BM	73.4	TA	4w	2	1368	0.15	0.0002
				GC	4w	18	3234	0.56	0.0018
				TA	—	0	2120	0.00	0.0000
				GC	—	4	3505	0.11	0.0004
4	5	GFP$^+$ BM	43.4	TA	8w	5	1581	0.32	0.0005
				GC	8w	24	3093	0.78	0.0024
				TA	—	2	1304	0.15	0.0002
				GC	—	0	4658	0.00	0.0000
14	5	GFP$^+$ BM	46.7	TA	10w	13	1564	0.83	0.0013
				GC	10w	44	1378	3.19	0.0044
				TA	—	0	1150	0.00	0.0000
				GC	—	1	2634	0.04	0.0001
73	9	GFP$^+$ BM	77.7	TA	10w	1	1044	0.10	0.0002
				GC	10w	0	3171	0.00	0.0000
				TA	—	0	1138	0.00	0.0000
				GC	—	0	556	0.00	0.0000
84	9	GFP$^+$	42.7	TA	3w	2	1205	0.17	0.1000
		BM-SP/CD45$^+$		TA	—	0	1189	0.00	0.0000
106	9	GFP$^+$	22.9	TA	3w	3	767	0.39	0.1500
		BM-SP/CD45$^+$		TA	—	0	773	0.00	0.0000
61	9	GFP$^+$	92.9	TA	10w	18	735	2.45	0.7965
		BM-SP/CD45$^+$		GC	10w	12	1176	1.02	0.5310
				TA	—	0	584	0.00	0.0000
				GC	—	4	2071	0.19	0.1770
69	9	GFP$^+$	10.4	TA	10w	0	405	0.00	0.0000
		BM-SP/CD45$^+$		GC	10w	7	2838	0.25	0.3500
				TA	—	0	1024	0.00	0.0000
				GC	—	1	2889	0.03	0.0500

[a] CTX was injected more than 12 weeks after transplantation. Mice were sacrificed 3, 4, 8, or 10 weeks after CTX injection.
[b] % = (the number of GFP$^+$ myofibers/the total number of myofibers per muscle section) × 100.
[c] % = (the number of GFP$^+$ myofibers/the number of transplanted cells) × 100.

muscles (Figs. 2F–G and I–J). To characterize SP cells in muscles, they were further fractionated by CD45 and GFP expression. GFP$^+$ SP/CD45$^+$ cells significantly increased in number in injured muscles, when compared with uninjured muscles (Figs. 2H and K). In both uninjured and injured muscles, GFP$^+$ SP cells were

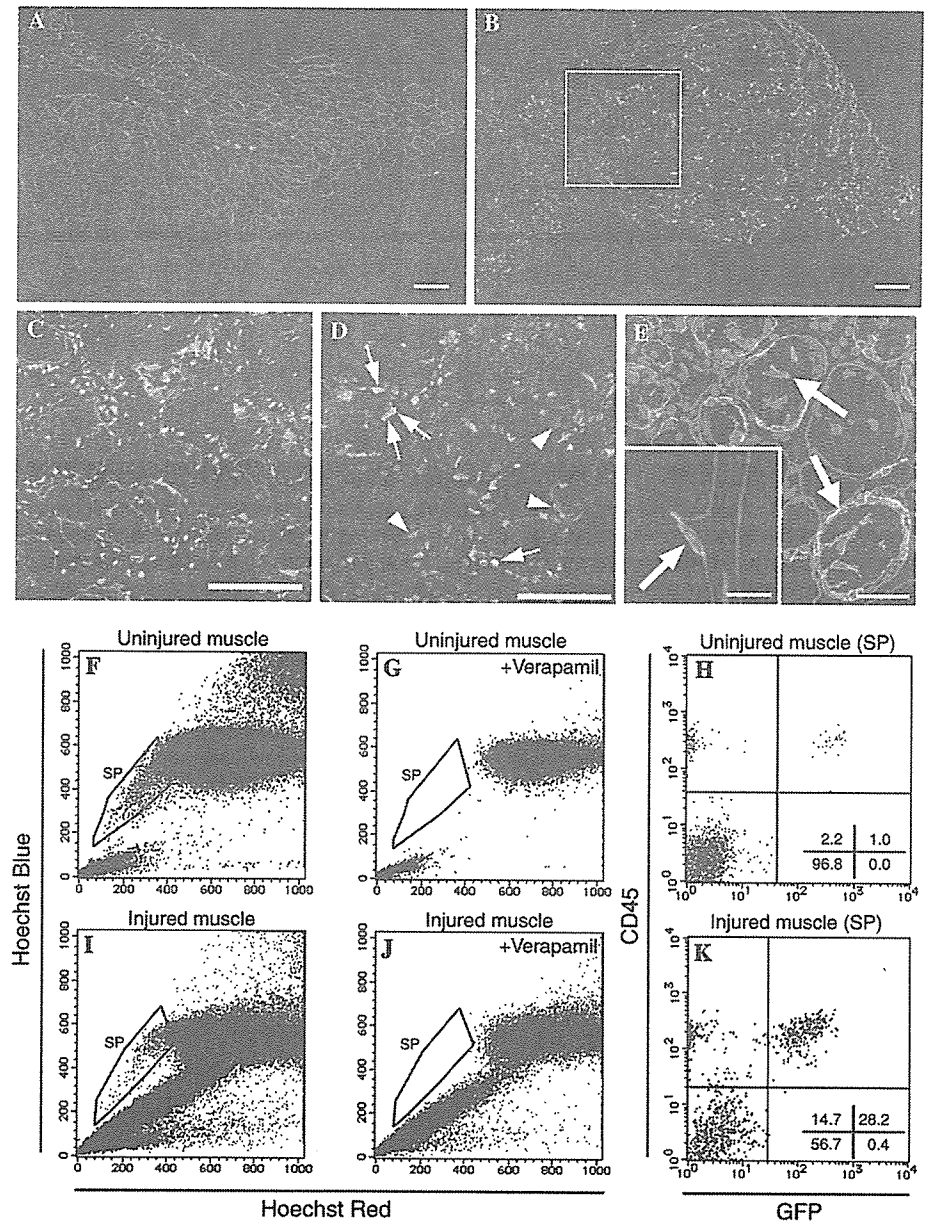

Fig. 2. Migration of BM-derived SP cells to regenerating skeletal muscle. (A,B) Immunofluorescent staining for GFP (green) and laminin α2 (red) of TA muscle cross-cryosections from GFP$^+$ BM-SP/CD45$^+$ cell-transplanted mice. (A) Only a few GFP$^+$ mononucleated cells were observed in intact muscle. (B) In contrast to (A), a great number of GFP$^+$ mononucleated cells have infiltrated into damaged muscle at 3 days after CTX injection. (C) A high magnification photograph of the inset area of (B), displaying triple immunofluorescent staining for GFP (green), laminin α2 (red), and nuclei (blue). GFP$^+$ cells were located in intra- and extra-basement membranes. (D) At 3 days after CTX injection, a cryostat section of regenerating muscle of a mouse transplanted with GFP$^+$ BM-SP/CD45$^+$ cells was stained with anti-Mac-1 antibody (red) and anti-GFP antibody (green). Nuclei were stained with TOTO3 (blue). Arrows indicate both GFP$^+$ and Mac-1$^+$ positive cells. Arrowheads indicate GFP$^+$ but Mac-1$^-$ cells. (E) A cryostat section of regenerating muscle at day 3 after CTX injection was stained with anti-M-cadherin antibody (green) and anti-laminin α2 antibody (red). Nuclei were stained with TOTO3 (blue). Arrows indicate M-cadherin$^+$ activated satellite cells. Our anti-M-cadherin antibody specifically recognized a satellite cell beneath the basement membrane in control muscle (arrow in inset of E). (F–K) Representative FACS analyses demonstrating that mononucleated cells isolated from uninjured muscles (F–H) or regenerating muscles (I–K) of GFP$^+$ BM-SP/CD45$^+$ cell-transplanted mice contained Verapamil-sensitive SP cells. These SP cells were further characterized with GFP and CD45 expression (H,K). Note that the percentage of a subfraction of SP cells expressing both GFP and CD45 was considerably increased at 3 days after CTX injection. In contrast, BM-derived SP cells expressing GFP but not CD45 were hardly detected in both regenerating and undamaged muscles. BM-GFP chimerisms of transplanted mice shown here were 93% (F–H) and 60% (I–K), respectively. Three uninjured mice and nine injured mice were analyzed and showed a similar tendency (data not shown). Bars, 100 μm in (A–D), 40 μm in (E), and 8 μm in inset of (E).

largely CD45$^+$ (Figs. 2H and K). Moreover, in GFP$^+$ BM-transplanted mice with more than 95% chimerism, nearly 100% of GFP$^+$ cells were CD45$^+$ (Uezumi et al., unpublished data), in agreement with previous reports [6,21,23]. We, therefore, selected CD45$^+$ cells to pursue the fate of BM-derived cells after muscle injury.

Table 2
GFP-chimerism in peripheral blood of transplanted mice

Number of transplanted mice	Transplanted cell[a]	Number of transplanted cells	GFP-chimerism in PB (%)[b]
3	GFP$^+$ SP/CD45$^+$	3000	0.09-0.32

[a] Transplanted cells were prepared from CTX-injected muscles (day 3) of *GFP* transgenic mice.
[b] GFP-chimerism in peripheral blood (PB) was determined at 4 weeks after transplantation.

Failure of BM-derived SP cells isolated from regenerating muscles to reconstitute the blood system of recipient mice

We observed that a large number of SP cells migrated from BM to muscles following injury. To directly examine whether migrated BM-derived SP cells in regenerating muscles had hematopoietic ability or not, we transplanted 3000 freshly isolated BM-derived SP/CD45$^+$ cells from regenerating muscles of *GFP* transgenic mice into lethally irradiated recipient mice ($n = 3$). Less than 1% of the peripheral blood cells of recipient mice were donor-derived GFP$^+$ blood cells 4 weeks after transplantation (Table 2), indicating that BM-derived SP cells in regenerating muscle contained very few or no hematopoietic stem and/or progenitor cells.

Analysis of surface marker expression on BM-derived SP cells

Previous studies showed that BM-SP cells and BM-derived SP cells in uninjured muscles possess hematopoietic potential [16–18,20]. However, our transplant studies suggested that BM-derived SP/CD45$^+$ cells in regenerating muscles were different from HSCs even if they had the SP phenotype. To compare the surface marker expression, we isolated three different SP cells, BM-SP cells, BM-derived SP cells of uninjured muscles, and BM-derived SP cells of injured muscles. They were labeled with antibodies to CD45 and one of the following markers: Sca-1, c-kit, CD34, or Mac-1 (Fig. 3A). We detected all markers on BM-SP cells, and their expression levels were similar to previous reports [16–18,28]. We observed a small percentage of c-kit$^+$ cells in the BM-derived uninjured muscle SP cells (Fig. 3A). However, importantly there were no c-kit$^+$ BM-derived SP cells in injured muscles (Fig. 3A).

Interestingly, BM-derived SP cells contained Mac-1^{low} cells in both injured and uninjured muscles (Figs. 3A, C, and E). These BM-derived SP/CD45$^+$ Mac-1^{low} cells in day 3 CTX-injected muscles increased in numbers (by muscle weight) approximately 18-fold, compared with uninjured muscles. We found that BM-derived SP/Mac-1^{low} cells were not labeled with anti-F4/80 antibody, which is a specific and sensitive marker for mature mouse macrophages (data not shown). In contrast, BM-derived Mac-1^{high} cells were fallen into the MP fraction (Figs. 3B–E) and expressed F4/80 antigen (data not shown). These results suggest that SP/CD45$^+$ Mac-1^{low} cells actively migrated from BM to injured muscles and that they were not mature myeloid cells.

Myogenic differentiation of BM-SP cells and BM-derived SP cells isolated from regenerating muscle

To analyze the cellular mechanism of myogenic differentiation of BM-SP cells and BM-derived SP cells from regenerating muscles in vitro, we first co-cultured BM-SP/CD45$^+$ cells from *GFP* transgenic mice with activated satellite cells of C57BL/6 mice. We found that GFP$^+$ BM-SP cells formed multinucleated myotubes (Fig. 4A). These myotubes expressed desmin and sometimes spontaneously contracted (data not shown). To determine whether BM-SP/CD45$^+$ cells fuse with host myogenic cells or not, we co-cultured BM-SP/CD45$^+$ cells prepared from *GFP* transgenic mice with activated satellite cells derived from Rosa26 mice, which express β-galactosidase (β-Gal) under a ubiquitous regulatory element [37]. X-gal staining showed that GFP$^+$ myotubes expressed β-Gal, indicating that BM-SP cells fused with co-cultured host myogenic cells and formed heterokaryotic myotubes (Figs. 4B and C). When GFP$^+$ BM-SP/CD45$^+$ cells were cultured alone in the differentiation medium or in the conditioned medium prepared from myogenic cells, they did not form GFP$^+$ myotubes (data not shown), suggesting that BM-SP/CD45$^+$ cells formed myotubes via cell-to-cell contact with myogenic cells.

Next, we examined whether migrated BM-derived SP cells isolated from regenerating muscles differentiated into skeletal muscle cells in vitro or not. We focused on Mac-1 expression of BM-derived SP cells because the results, shown in Fig. 3, indicated that considerably greater number of BM-derived Mac-1^{low} SP cells infiltrated into injured muscles than into uninjured muscles. In addition, it has been recently reported that monocytes differentiate into various cell types in certain culture conditions [39]. We fractionated BM-derived cells prepared from *GFP* transgenic mouse muscles damaged by CTX injection based on both Mac-1 expression and SP phenotype: SP/CD45$^+$ cells, SP/CD45$^+$ Mac-1$^-$ cells, SP/CD45$^+$ Mac-1^{low} cells, MP/CD45$^+$ cells, MP/CD45$^+$ Mac-1^{low} cells, and MP/CD45$^+$ Mac-1^{high} cells. Then each fraction was co-cultured with activated satellite cells from C57BL/6 mice. After 14 days of co-culture, they were fixed and stained with anti-GFP antibody

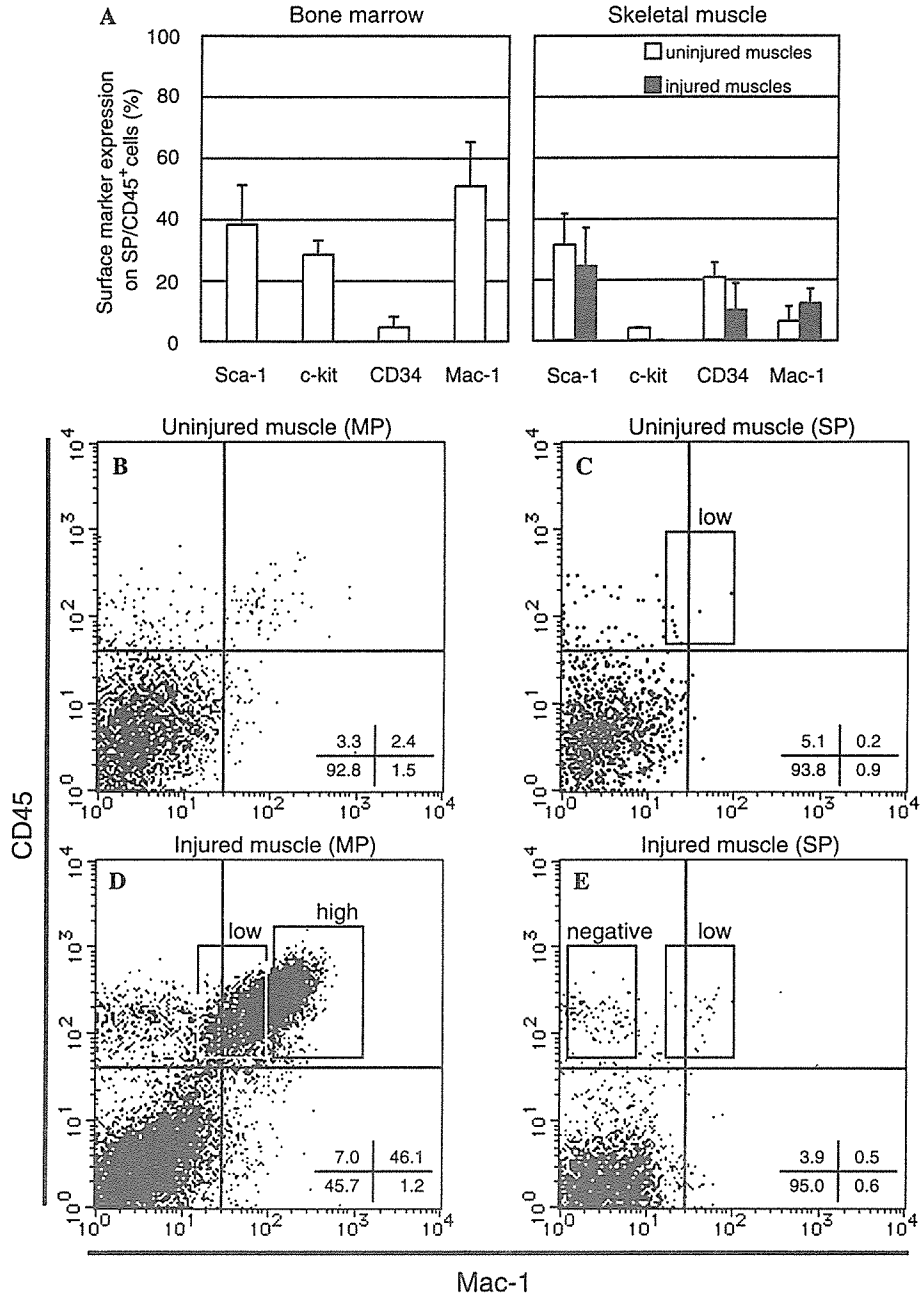

Fig. 3. Analysis of surface marker expression on BM-derived SP/CD45$^+$ cells prepared from muscles. (A) SP cells from BM (left graph), BM-derived SP cells from uninjured (white columns in right graph), and BM-derived SP cells from injured muscles (black columns in right graph) were isolated and then stained with anti-CD45 antibody and one of the following markers: Sca-1, c-kit, CD34, or Mac-1. The percentages of surface marker expression on BM-SP/CD45$^+$ cells (left graph) and on BM-derived SP/CD45$^+$ cells (right graph) were calculated by the following formula: (%) = 100 × (the number of surface marker-positive CD45$^+$ cells in the SP fraction)/(the number of CD45$^+$ cells in the SP fraction). Note that the expression of c-kit in BM-derived SP/CD45$^+$ cells from injured muscles was not at a detectable level. All values (means ± SD) are based on at least three separate experiments. (B–E) Representative FACS analysis demonstrating that mononucleated cells in the MP fraction (B,D) or the SP fraction (C,E) isolated from uninjured muscles (B,C) or injured muscles (D,E) of the *GFP* transgenic mice. In injured muscles, MP/CD45$^+$ cells expressed Mac-1 with a broad range of intensities (D). By contrast, the SP fraction from injured muscles contained not CD45$^+$ Mac-1^{high} cells but CD45$^+$ Mac-1^{low} cells (E). Importantly this SP/D45$^+$ Mac-1^{low} fraction increased in cell number as well as in ratio after muscle injury (rectangles marked "low" in C,E; also see A). The SP sub-fractions shown by rectangles in (D,E) were isolated and then used in further culture experiments (see Fig. 4 and Table 3).

and anti-sarcomeric α-actinin antibody (Figs. 4D–F). BM-derived SP cells gave rise to myotubes more effectively than BM-derived MP cells (Table 3). In particular, the BM-derived SP/CD45$^+$ Mac-1^{low} fraction was highly concentrated in cells capable of myotube formation (Table 3). More importantly, sarcomeric α-actinin-expressing mononucleate myocytes were observed in our co-culture system (Figs. 4G–J), indicating that